Journal of
Materials Chemistry A

Materials for energy and sustainability

Accepted Manuscript

This article can be cited before page numbers have been issued, to do this please use: W. Yang, J. Zeng, A. Lang, K. Zhou, W. Yang and X. Peng, *J. Mater. Chem. A*, 2025, DOI: 10.1039/D5TA05279C.

ROYAL SOCIETY OF CHEMISTRY

rsc.li/materials-a

Biomass-based separators for aqueous zinc-ion batteries: advantages, strategies, and perspectives

View Article Online
DOI: 10.1039/D5TA05279C

Wang Yang, Jiaming Zeng, Aoxue Lang, Keyu Zhou, Wu Yang, Xinwen Peng*

Dr. Wang Yang, J. Zeng, A. Lang, K. Zhou, Dr. Wu Yang, Prof. X. Peng
State Key Laboratory of Advanced Papermaking and Paper-based Materials
School of Light Industry and Engineering
South China University of Technology
Guangzhou 510641, China
E-mail: yangw5@scut.edu.cn

Abstract

Aqueous zinc-ion batteries (ZIBs) have emerged as a promising candidate for large-scale energy storage owing to their intrinsic safety, low cost, and environmental friendliness. Currently, ZIBs have achieved significant advancements in core components such as cathode, anode, and electrolyte, whereas research progress on separator materials remains comparatively limited. The separator, as a crucial component of ZIBs, plays a crucial role in preventing internal electrical short circuits and facilitating ion transport. Biomass-based separators (e.g., cellulose, chitosan, chitin, and lignin) offer eco-friendly advantages by utilizing renewable resources with tunable microstructures and abundant functional groups, enabling enhanced wettability, mechanical strength, and dendrite suppression, thereby improving battery safety and performance. In this review, we summarize the recent advances of biomass-based separators for application in aqueous ZIBs. We begin with a comprehensive overview of ZIBs separators and their fundamental requirements. Then, we systematically analyze representative biomass-based separators for ZIBs, focusing on their structural configurations, preparation methods, modification strategies, and operational mechanisms (including regulating the uniform Zn deposition, inhibiting the Zn dendrites growth, and avoiding side reactions). Finally, the remaining challenges and promising perspectives of biomass-based separators for ZIBs are outlined, providing helpful guidance for their further development in large-scale applications.

Keywords: Biomass materials; Sustainability; Ion transport; Zn dendrites; Zinc-ion batteries; Separators

View Article Online
DOI: 10.1039/D5TA05279C

1. Introduction

Aqueous ZIBs have received considerable attention as an emerging electrochemical energy storage system in recent years due to their high theoretical capacity (820 mAh g^{-1}, 5855 mAh cm^{-3}), low redox potential (−0.76 V vs. standard hydrogen electrode), intrinsic safety associated with aqueous electrolytes, and low cost.[1-3] The ZIBs system primarily consists of an anode, cathode, electrolyte, and separator, and its working principle is illustrated in Fig. 1a. The hydrogen evolution reactions (HER) and corrosion reactions originating from the free water molecules and electrolyte decomposition disturb both the electric field and ion distribution at the zinc deposition interface, leading to the non-uniform Zn deposition and finial Zn dendrites, which can penetrate the separator and cause short circuits.[4] As a critical component in ZIBs, the separator serves two essential roles in the battery: isolating the positive and negative electrodes to prevent short circuits while maintaining good interfacial contact, and providing rapid transport channels for ion transport.[5] Although the separator does not directly participate in electrochemical reactions of ZIBs, its structure and properties can regulate electrolyte distribution, suppress Zn dendrites formation, and enhance cycle stability/longevity.[6-8] Therefore, the design and selection of the separator are crucial for achieving optimal electrochemical performance in ZIBs.

Currently, the most commonly used commercial separator for ZIBs is glass fiber (GF) separators, possessing high porosity and electrolyte wettability. However, their large pore size (micron scale) and irregular pore structure accommodating a large number of SO_4^{2-} and H^+ ions trigger side reactions and non-uniform Zn^{2+} flux, accelerating dendrites formation.[9] Their poor mechanical strength renders them susceptible to penetration by Zn dendrites during repeated cycling, leading to the internal short circuits and safety risks.[10] Moreover, the production process of GF separators is relatively complex, raising environmental concerns. Recent studies reveal that surface modification of GF separators has proved to be a promising strategy for improving electrochemical properties, which can be categorized into three key aspects: First, modified surfaces with optimized pore structures and zincophilic functional groups effectively regulate Zn^{2+} flux distribution, thereby suppressing Zn dendrites growth; Second, advanced coatings such as inorganic ceramic layers or polymer-based films demonstrate superior electrolyte wettability and serve as robust physical barriers to eliminate side reactions; Third, the introduction of negatively charged functional groups through surface modification can repel SO_4^{2-}, thereby reducing byproduct formation. However, their high cost and excessive thickness (typically >300 μm) hinder energy density and scalability of ZIBs.[11]

In recent years, biomass materials (e.g., cellulose, chitosan, chitin, and lignin) have emerged

View Article Online
DOI: 10.1039/D5TA05279C

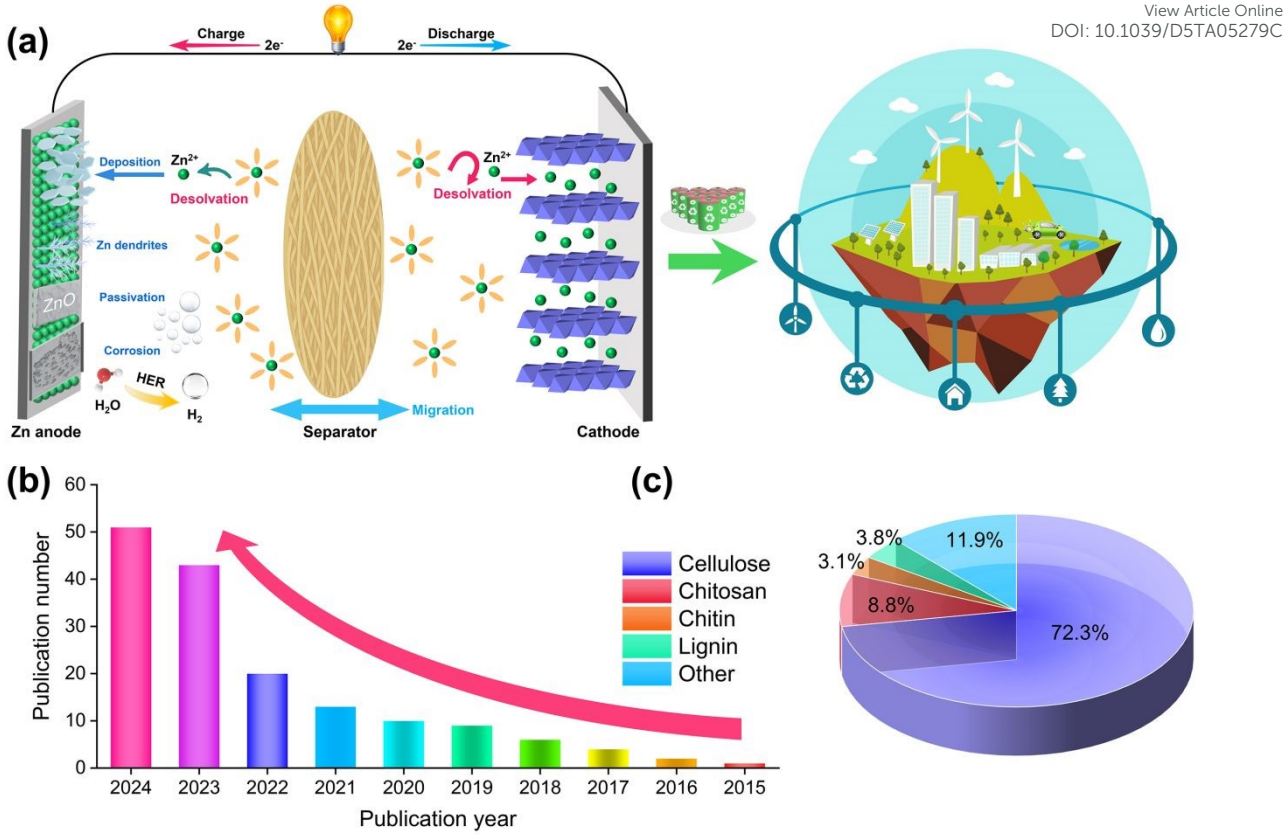

Fig. 1. (a) Schematic illustrations for the structure and working principle of ZIBs. (b) Number of publications over the past decade devoted to biomass-based separators for ZIBs. (c) Distribution of publications over the past decade regarding the different biomass materials as separator for ZIBs.

as promising alternative candidates for ZIBs separators (Fig. 1b). Not surprisingly, cellulose is the more widely used biopolymer as separator for ZIBs (Fig. 1c). Beyond their inherent biodegradability and sustainability derived from renewable sources, these biomass-based separators offer distinct advantages including tunable microstructures and abundant functional groups, which collectively contribute to superior wettability, enhanced mechanical strength, and dendrite suppression. Specifically, their intrinsic polar functional groups (–OH, –COOH, and $–NH_2$) provide abundant binding sites, thus reshaping the Zn^{2+} solvation structure and promoting uniform Zn nucleation/deposition.[12] In addition, the hierarchical porous structures of biomass-based separators can effectively regulate Zn^{2+} flux, and targeted chemical modification of biomass materials can significantly improve their mechanical strength and electrochemical stability.[13] Nevertheless, several challenges remain to be addressed for the practical application of biomass-based separators, such as ensuring sufficient mechanical strength, optimizing the pore structure for rapid ion transport, and maintaining compatibility with aqueous electrolytes.

To our knowledge, recent reviews on separators of ZIBs provide a comprehensive overview

View Article Online
DOI: 10.1039/D5TA05279C

of advanced design strategies focused on functionalized architectural design and chemical modification for dendrite suppression and interfacial stability enhancement. However, there is still a lack of comprehensive discussion regarding the advantages and challenges of biomass-based separators compared with GF separators, especially the underlying mechanisms and large-scale applications. This review provides an in-depth examination of the recent achievements in biomass-based separators for ZIBs, highlighting fundamental requirements, structural configurations, preparation methods, and modification strategies. We also present the classification, summary, and discussion of biomass-based separator work from the perspective of similar modification methods and operational mechanisms. Finally, the remaining challenges and future development directions of biomass-based separators for ZIBs are summarized and analyzed to promote further research and development in large-scale applications.

2. Why Use Biomass Materials for ZIBs separators?

The rapid advancement of energy storage technologies, driven by the development of electric vehicles and the acceleration of portable electrical devices, has propelled significant breakthroughs in battery separators.[14] Currently, GF separators are the predominant choice at the laboratory level, which can meet the fundamental requirements of ZIBs. However, GF separators are not suitable for mass production due to their high cost, complex manufacturing processes, and poor mechanical properties.[15] Therefore, the exploitation of advanced separators has emerged as a critical research frontier to address the limitations of conventional GF separators in ZIBs. Biomass-based separators are a promising alternative to traditional separator technologies owing to their inherent sustainability, cost-effectiveness, and multifunctional structural advantages. Fig. 2 provides a comprehensive overview of the biomass source, synthesis, and advantages of biomass-based separators for ZIBs in recent years, which have been discussed and summarized in the subsequent sections.

2.1 Fundamental Requirements for Separators

The characteristics of separators significantly determine the interfacial structure and internal resistance of ZIBs, which will greatly affect overall battery performance including the cycling stability, lifespan, and safety.[16] Consequently, this section will introduce and discuss several key characteristics of separators.

Firstly, the separator needs to be chemically and thermally stable to ensure long-term operational stability and durability, preventing dendrite-induced short circuits and maintaining structural integrity under varying temperature conditions and working environments. Specifically, the separator should not react with the electrodes or electrolyte and must remain

View Article Online
DOI: 10.1039/D5TA05279C

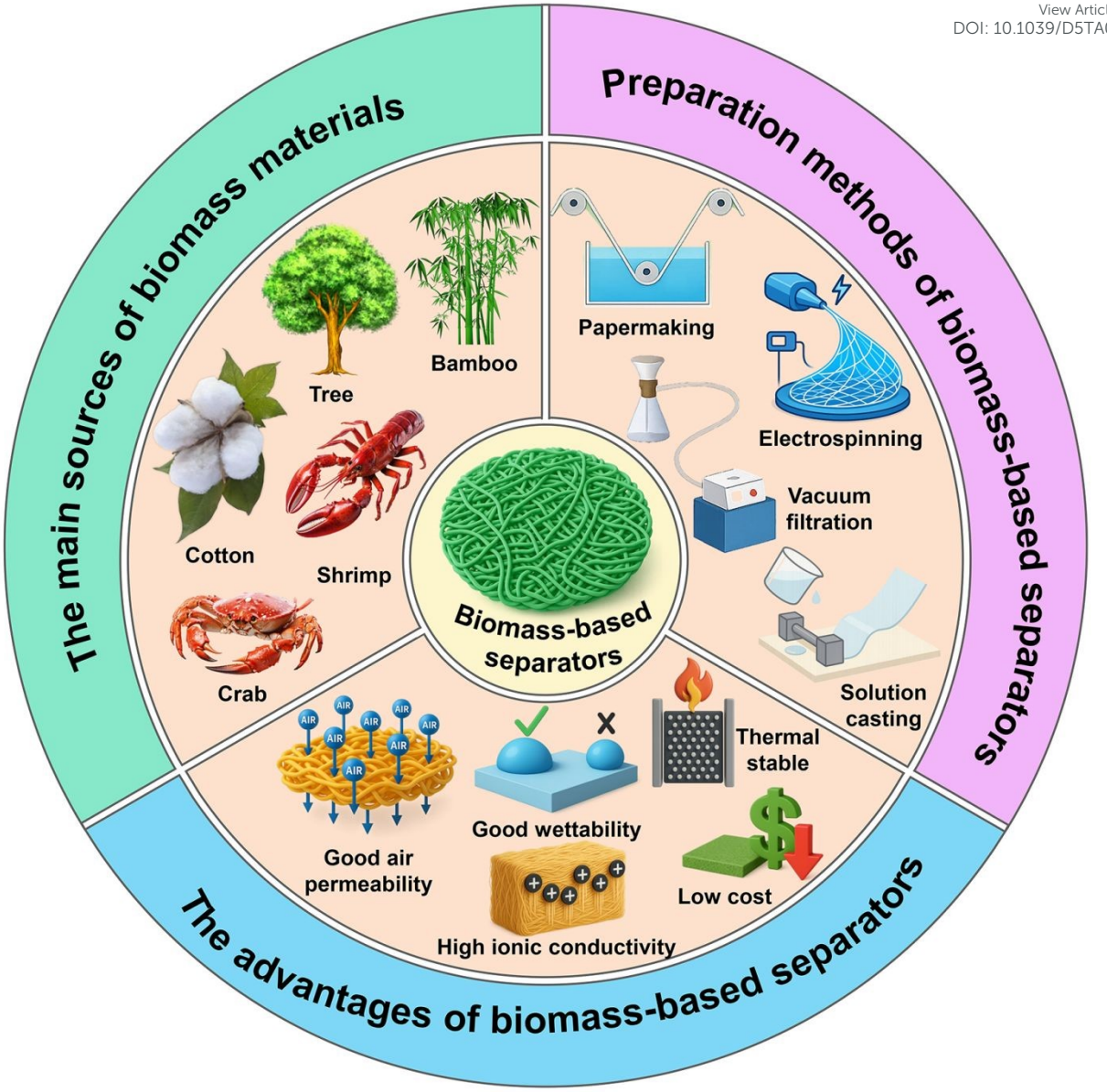

Fig. 2. Overview of biomass-based separators for ZIBs.

stable when immersed in electrolyte solutions for long operational periods (>10 years). Furthermore, the thermal shrinkage of the separator should not exceed 1% after 1 h of exposure to 140 ºC.[17] Secondly, thickness and mechanical properties are critical parameters of the separator that significantly influence battery performance and safety. A thinner separator can reduce internal resistance, shorten ion migration pathways, and improve the volumetric energy density, but it exhibits lower mechanical strength and is susceptible to mechanical breakage.[18] Therefore, the thickness of the separator should be as thin as possible while maintaining sufficient mechanical strength. The mechanical properties of the separator primarily include puncture strength and tensile strength. It must simultaneously withstand the piercing forces of Zn dendrites during battery operation and endure manufacturing-associated stresses including puncture, wear, compression, and tensile deformation.[6]

View Article Online
DOI: 10.1039/D5TA05279C

Meanwhile, the porosity of the separator is another critical parameter that fundamentally determines its permeability and ionic conductivity.[19] It is defined as the percentage of the internal pore volume relative to the total separator volume, and the porosity of commercial separators ranges from 40% to 60%. Generally, a higher porosity in separators correlates with enhanced permeability and ionic conductivity, thus improving the electrochemical performance of ZIBs.[5] However, excessive porosity can compromise the mechanical strength of the separator. Furthermore, the pore size of the separator significantly influences ion transport within the electrolytes. Specifically, the pore size of the separator must be smaller than the particle size of the electrode active materials to effectively prevent the particles from reaching the opposite electrode, as well as avoid the deposition of Zn in the pores.[20] Conversely, the large pore size of the separator can accelerate the self-discharge process of ZIBs. Therefore, an optimal porosity and pore size of the separator must be selected for practical applications. In addition, the electrolyte wettability of the separator should be good, thus guaranteeing effective electrolyte infiltration and ion transport. High electrolyte wettability facilitates the uniform distribution of electrolyte inside the battery, which is crucial for maximizing ionic conductivity and overall battery performance.[21] The electrolyte wettability of the separator can be assessed by measuring the electrolyte diffusion height or the contact angle. An increased electrolyte diffusion height and a reduced contact angle indicate improved surface affinity and wettability. Conversely, poor electrolyte wettability of the separator would increase internal resistance, influencing the rate performance of ZIBs.[22]

The ionic conductivity and ion transference number of the separator are two significant electrochemical parameters, which greatly influence the overall battery performance. These electrochemical parameters also have a great impact on the uniform deposition of Zn anodes.[6] The ionic conductivity of the separator reflects ionic mobility of the electrolyte within its porous structure under an electric field, which can be measured by electrochemical impedance spectroscopy (EIS) according to the following equation:

$$\sigma = \frac{d}{(R_b \times A)} \quad \text{(Eq.1)}$$

where R_b is the bulk resistance, d and A are the thickness of the separator and the contact area between the stainless steel electrode and the separator, respectively.

Previous studies have demonstrated that the ionic conductivity of a separator is influenced by its surface chemistry and microstructure characteristics, including porosity (ε) and tortuosity (τ).[23] Therefore, it is anticipated that high ionic conductivity in separators can be achieved through strategic surface modifications and structural optimizations, such as tailored porosity distribution and hierarchical pore architectures. The relationships among these parameters are

View Article Online
DOI: 10.1039/D5TA05279C

defined by equations (Eq. 2-4):

$$N_M = \frac{\sigma_b}{\sigma} \quad \text{(Eq.2)}$$

$$\sigma = \sigma_b \frac{\varepsilon}{\tau^2} \quad \text{(Eq.3)}$$

$$\tau = \left(\frac{L_{pore}}{d}\right)^2 \quad \text{(Eq.4)}$$

where N_M is McMullin Number, σ_b is the ionic conductivity of liquid electrolyte, σ is ionic conductivity of liquid electrolyte-filled separator, L_{pore} is the shortest distance through the pore system, and d is the thickness of the separator.

The ion transference number (t), defined as the fraction of total charges carried by a specific ion in an electrolyte (Eq.5), is a critical parameter for evaluating the efficiency of ionic mobility in separator.[24] The principle underlying this measurement involves the movement of ions through the electrolyte under the influence of electric fields, which is affected by factors such as temperature, concentration, and the structural properties of the separator. The cationic transference number can be quantified using the constant potential polarization method, and calculated according to Eq. 6. The high ionic transference number of Zn^{2+} in ZIBs demonstrates a superior permeability of Zn^{2+} through the separator compared to anionic species, facilitating more efficient participation in electrochemical reactions at the Zn anode interface and promoting the uniform Zn deposition.

$$t_+ = \frac{Q^+}{Q^+ + Q^-} \quad \text{(Eq.5)}$$

$$t_+ = \frac{I_{ss}(\Delta V - I_0 R_0)}{I_0(\Delta V - I_{ss} R_{ss})} \quad \text{(Eq.6)}$$

where Q^+ and Q^- are charges carried by cations and anions, respectively. I_0 and R_0 are the initial current and resistance , respectively. I_{ss} and R_{ss} are the steady state current and resistance , respectively. ΔV is constant potential.

Finally, the cost of the separator is also an important factor, accounting for 10%−20% of the total cost of the batteries.[25] Traditionally, the separator originated from petroleum-based polymers are widely used, but their high production costs and environmental concerns have prompted the exploration of alternative materials. The utilization of naturally abundant biopolymers presents a sustainable alternative for separator fabrication that also addresses sustainability issues.[26] These natural biomass materials not only reduce dependency on nonrenewable resources but also lower manufacturing costs, making them attractive for large-scale applications. Therefore, it is essential to develop a high-performance, safe, low-cost, and environmentally friendly separator through a straightforward and controllable manufacturing process.

Overall, the separators for ZIBs should meet the following requirements beyond the general

View Article Online
DOI: 10.1039/D5TA05279C

functions: 1) enhance pore size homogeneity and spatial arrangement to ensure the uniform electric field distribution and Zn^{2+} flux; 2) precise regulate the Zn^{2+} solvation sheath through selective interactions (e.g., electrostatic anchoring, hydrogen bonding), thereby reducing activation energy for Zn deposition and suppressing Zn dendrites formation; 3) strong ion-selectivity to prevent cathodic dissolution and inhibit undesired ion shuttling between electrodes.

2.2 Preparation Methods of Biomass-based Separators

The preparation methods for biomass-based separators are crucial for optimizing their properties, including microstructure, mechanical strength, porosity, pore size, and interfacial compatibility, as well as enhancing cost-effectiveness in ZIBs. Currently, the primary techniques employed to produce separators from natural polymers include solution casting, vacuum filtration, phase separation, electrospinning, and papermaking.[27] Each method offers distinct advantages and challenges, influencing the separator's properties such as thickness, porosity, and permeability. Consequently, the development of scalable and efficient preparation methods is essential for the successful integration of biomass-based separators into ZIBs. This section summarizes the prevalent preparation methods for biomass-based separators and discusses future directions to overcome current challenges.

Solution casting and vacuum filtration are widely used methods for preparing biomass-based separators due to their simplicity, scalability, and cost-effectiveness. Typically, biomass materials such as cellulose, chitin, lignin, and their derivatives are dissolved or dispersed in appropriate solvents to form homogeneous suspensions through mechanical dispersion or chemical modification, which are then cast onto substrates or filtered to form thin membranes. These techniques enable precise control over thickness and uniformity of the separator, which is essential for achieving consistent ion transport pathways and mechanical integrity. For example, bacterial cellulose (BC) membranes are fabricated by vacuum filtration of BC nanofiber suspensions, forming a dense and porous network that enhances mechanical strength and electrolyte wettability.[28] Similarly, TEMPO-oxidized chitin nanofibers (TCh) are cast into flexible membranes via solution casting methods, in which polar functional groups (−COOH, −OH) promote Zn^{2+} desolvation and facilitate uniform Zn deposition.[29] Although these methods are simple and scalable, they require optimization of solvent systems to balance viscosity and uniformity, which ensures a porous network with superior electrolyte uptake and ionic conductivity. Besides, accurate control of drying temperature, solution concentration, and other processing parameters are essential for optimal separators.

Electrospinning has emerged as a powerful technique for fabricating nanofibrous biomass-

View Article Online
DOI: 10.1039/D5TA05279C

based separators with appropriate thickness, high porosity, interconnected pore networks, and large pore size. In this process, a high-voltage electric field is applied to a polymer solution or melt, and the ejecting ultrafine fibers formed a conical shape (i.e., "Taylor cone") are collected as nonwoven mats.[30] The morphology and properties of electrospun membranes can be easily adjusted by controlling various aspects of the preparation process, including composition, solution concentration, flow rate, voltage, distance, extrusion rate, and syringe size.[31] Biomass materials such as cellulose nanofibers, chitosan, and lignin derivatives have been successfully electrospun into membranes, demonstrating enhanced electrolyte wettability and rapid ion transport. Chen et al.[32] employed the electrospinning method for the preparation of a modified cellulose acetate (MCA) membrane. The modified MCA membrane exhibited good chemical stability and superior wettability. Notably, the porous and three-dimensional (3D) network structure of electrospun membranes facilitates rapid Zn^{2+} diffusion and mitigates dendrite growth by homogenizing ion flux. Furthermore, electrospinning allows for the easy incorporation of functional additives, such as conductive polymers or inorganic nanoparticles, thus tailoring the properties of the separators (such as composition, structure, thermal stability, mechanical strength, and wettability). Nevertheless, challenges remain in achieving uniform fiber morphology and mechanical properties, especially under prolonged cycling.

The papermaking process is a well-established method for fabricating cellulose-based separators. This technique involves the suspension of cellulose fibers in an aqueous medium, followed by the formation of paper on a mesh scaffold, which facilitates precise control over nanofiber alignment, porosity, and functional group distributions. The papermaking method offers several advantages, including high porosity, flexibility, and biodegradability, thereby enhancing battery performance and safety. Moreover, this method is cost-effective, environmentally friendly, and scalable for industrial production. For instance, Ge et al.[33] successfully fabricated CNF-SO_3Zn separators on a large scale using traditional papermaking techniques, achieving superior preferred Zn^{2+} conductivity and hydrophilicity. It is crucial to further explore the scalability of the papermaking process and understand its environmental implications, determining the commercial feasibility of the industry. Consequently, biomass-based separators fabricated via the papermaking method play a vital role in the development of sustainable ZIBs. Future research should focus on optimizing pore architecture, exploring multifunctional coatings, and elucidating the ion transport mechanisms at molecular levels.

In a word, the currently commercialized preparation method is the papermaking process. This technique yields a cellulose separator with lower production costs compared to other methods, and has gained industry-wide recognition as viable options for mid-to-low-end battery

View Article Online
DOI: 10.1039/D5TA05279C

markets.[34] Although electrospinning appeared relatively late than papermaking, it has progressively emerged as the preferred method for advanced separator manufacturing owing to its simplicity. Despite inherent challenges in scalability and production efficiency, vacuum filtration technology has been adopted by some companies for the production of asymmetric separators for specialized battery applications.

2.3 Advantages of Biomass-based Separators

Recently, biomass has garnered significant attention as an alternative material for separators, which is widely used as the matrix or reinforced filler in ZIBs.[35] Their natural abundance, renewable, and eco-friendly characteristics contribute to sustainable development while lowering the raw material costs for separators. Therefore, biomass-based separators possess several advantageous properties, including high thermal stability, superior mechanical properties, and excellent electrolyte wettability.

2.3.1 Electrolyte Wettability

The wettability of the separator is characterized by three key parameters: the electrolyte diffusion time, adsorption capacity, and the contact angle formed between the electrolyte and the separator surface.[36] The olefin chains in polyolefin separators are hydrophobic, and their surface energy is not compatible with that of the aqueous electrolyte, leading to poor electrolyte wettability. In contrast, the inherent hydrophilic functional groups (e.g., hydroxyl and carboxyl groups) in biomass materials significantly improve interfacial compatibility with aqueous electrolytes, thereby reducing contact angles and facilitating rapid electrolyte infiltration.[37] The superior electrolyte wettability of biomass-based separators ensures a continuous ionic conduction pathway and minimizes interfacial resistance, resulting in high ionic conductivity. For instance, the Zr-CNF separators achieve high porosity and good electrolyte wettability, enabling uniform electrolyte distribution and enhanced Zn^{2+} transport kinetics.[38] The electrolyte wettability can be further incorporated by compositing hydrophilic nanomaterials (such as graphdiyne,[39] graphene oxide,[40] ZrO_2,[41] Ag[42] etc.) or grafting hydrophilic functional groups (such as sulfonate,[33] carboxymethyl,[43] amino[44] etc.). For example, Zhang et al.[44] introduce quaternary amine groups on the surface of nanocellulose fibers for the preparation of ZIBs separator. The amino-modified nanocellulose separator exhibits an enhanced electrolyte wettability, attributed to the higher hydrophilicity of cationic amine functional groups. However, these modification methods may lead to increased swelling of the biomass-based separator in the aqueous electrolyte, potentially damaging the overall structural integrity of the separator.

2.3.2 Thermal Stability

View Article Online
DOI: 10.1039/D5TA05279C

The thermal stability of the separator is critical for ensuring safe and reliable battery operation, especially under extremely high-temperature conditions. An effective separator must maintain its integrity to isolate the positive and negative electrodes, thereby mitigating the risk of short circuits. The conventional polyolefin separators suffer from a low glass transformation temperature and melting point, which results in significant shrinkages when exposed to the elevated temperatures (above 100 ºC).[45] Impressively, the biomass-based separators exhibit superior thermal stability, maintaining their structural integrity without deformation even at temperatures reaching 200 ºC.[46] This enhanced thermal stability is primarily attributed to the strong intermolecular hydrogen-bonding interactions and the inherent stability of the biomass materials, which help to prevent thermal degradation and maintain the mechanical properties of the separators. Consequently, biomass-based separators offer significant advantages in battery applications, which can effectively mitigate risks associated with thermal runaway and prolong the operational lifespan of ZIBs under high-power charging/discharging scenarios. Zheng et al.[42] reported an ultrathin Janus separator featuring the BC layer on one side and Ag nanowires/BC layer on the other side. This BC-based separator maintained stable pore structures and prevented zinc dendrite penetration even at 50 ºC during 500 cycles in ZIBs, suggesting their thermal resilience.

2.3.3 Air Permeability

The superior air permeability of the separator directly correlates with enhanced ionic conductivity, typically quantified by Gurley value. A higher air permeability generally indicates a more open and interconnected pore network, which facilitates the transport of electrolyte ions across the separator. This improved ion transport reduces resistance within the battery, thereby enhancing the ionic conductivity. The Gurley value represents the time required for a specific gas to pass through a defined area of the separator under specified pressure.[47] This value reflects the tortuosity of the pore structure, which can be measured using a gas permeability tester. Generally, a low Gurley value means excellent air permeability and high ionic transmission rate. The air permeability of the separator is influenced by several factors, including pore size, pore distribution, porosity, micropore shape, and tortuosity.[48] Compared with polyolefin separators, biomass-based separators demonstrate a smaller Gurley value and superior ion permeability, attributed to their favorable porosity and pore structure. Therefore, optimizing these characteristics is essential for improving the overall performance of the biomass-based separator.

2.3.4 Ionic Conductivity

View Article Online
DOI: 10.1039/D5TA05279C

The ionic conductivity of the separator plays a pivotal role in determining the electrochemical performance of ZIBs, including charging/discharging rates, power density, and energy efficiency. Conventional polyolefin separators are often limited by their low ionic conductivity due to their inherent hydrophobicity, which impedes electrolyte wetting and ion transport kinetics. In contrast, biomass-based separators demonstrate high ionic conductivity owing to their hierarchically interconnected porous architectures and hydrophilic characteristics, *thereby* enabling rapid Zn^{2+} diffusion. Moreover, the open and porous structure of biomass materials further enhances ion mobility, allowing for more efficient ion transport during battery operation.[49] For example, a wood-inspired anisotropic separator composed of nanofibrillated cellulose and chitosan exhibited an exceptional ionic conductivity of 20.5 mS cm^{-1} at a reduced thickness of 23 μm, while maintaining high modulus (7.3 GPa).[50] This superior performance primarily originates from its vertically aligned channels and low tortuosity, which minimizes ion diffusion barriers and homogenizes Zn^{2+} flux.

2.3.5 Cost

A separator is an inactive component in the ZIBs; thus, its cost should not constitute a significant proportion of the total cost. Biomass-based separators can be manufactured from abundant and renewable natural resources, rendering them an economically viable option for large-scale battery production. This inherent availability significantly reduces the raw material costs associated with separator production compared to commercial glass fiber or synthetic polymer separators. The utilization of agricultural/forestry waste and byproducts in the synthesis of these separators further improves their cost-effectiveness, significantly reducing feedstock costs by 60–80%. Moreover, the processing techniques for biomass-based separators can be optimized to minimize manufacturing expenses. Recent studies demonstrate that plant-derived cellulose separators can be fabricated at \$0.5–1.2/m^2, approximately 30–50% cheaper than conventional GF separators (\$1.8–2.5/m^2).[51]

3. Design Strategies for Biomass-based separators

The performance of the battery is greatly influenced by the characteristics and functions of the separator. The use of biomass materials for ZIBs separators provides significant advantages, including environmental sustainability, renewability, cost-effectiveness, tunable microstructures, and abundant functional groups. Currently, the design strategies for biomass-based separators can be classified into three categories: 1) Pure biomass separators, which utilize the inherent functional groups and adjustability properties of natural polymers in biomass to optimize the performance of ZIBs; 2) Biomass-based composite separators integrated with

View Article Online
DOI: 10.1039/D5TA05279C

organic or inorganic materials to enhance structural flexibility and ion transport efficiency.[3] Surface-functionalized coated separators, which employ cellulose as a functional substrate to enhance thermal stability and electrolyte affinity. In the following parts, we will introduce these three types of biomass-based separators, these biomass-based with the electrochemical performances for ZIBs are presented in Table 1.

3.1 Pure Biomass Separators

Biomass-derived natural polymers, inherently possessing abundant functional groups (–OH, –COOH, and $–NH_2$), can be directly utilized as separator matrices due to their intrinsic chemical reactivity. These functional groups facilitate robust coordination with electrolyte ions through Lewis acid-base interactions, thereby effectively modulating Zn^{2+} migration kinetics and the Zn deposition process. Moreover, chemical modification strategies can be implemented by exploiting the reactivity of these functional groups, further enhancing the Zn^{2+} transport and optimizing Zn deposition behavior.

3.1.1 Natural Biopolymer Separators

Cellulose, the most abundant natural biopolymer on Earth, serves as a cornerstone for sustainable materials engineering due to its biodegradability and renewability. Its chemical structure consists of a linear macromolecule formed by repeating β-D-glucopyranose units interconnected via β-(1→4) glycosidic bond, exhibiting abundant van der Waals and hydrogen bonding interactions.[52,53] This supramolecular architecture endows cellulose materials with remarkable mechanical strength and chemical stability.[54] Cellulose can be extracted from a wide range of natural plant sources, including cotton, flax, bamboo, and other lignocellulosic biomass. For instance, Zhou et al.[55] developed cotton-derived cellulose membranes as separators for aqueous ZIBs, demonstrating a remarkable capability to suppress Zn dendrite growth and mitigate harmful side reactions. This separator was fabricated using a simple filtration method, featuring a uniform nano-porous structure, abundant surface hydroxyl groups, and high ionic conductivity. As depicted in Fig. 3a, raw cotton materials were subjected to sequential $NaOH/H_2O_2$ pretreatment, effectively removing lignin and hemicellulose components. Subsequently, the resulting cellulose fibers (CF) were formed into CF separators through a vacuum filtration process, demonstrating excellent flexibility. It can be observed that the CF separator possessed densely packed, small-sized, and uniformly distributed internal pores compared to GF separator (Fig. 3b-c). The electrolyte wettability of the CF separator was

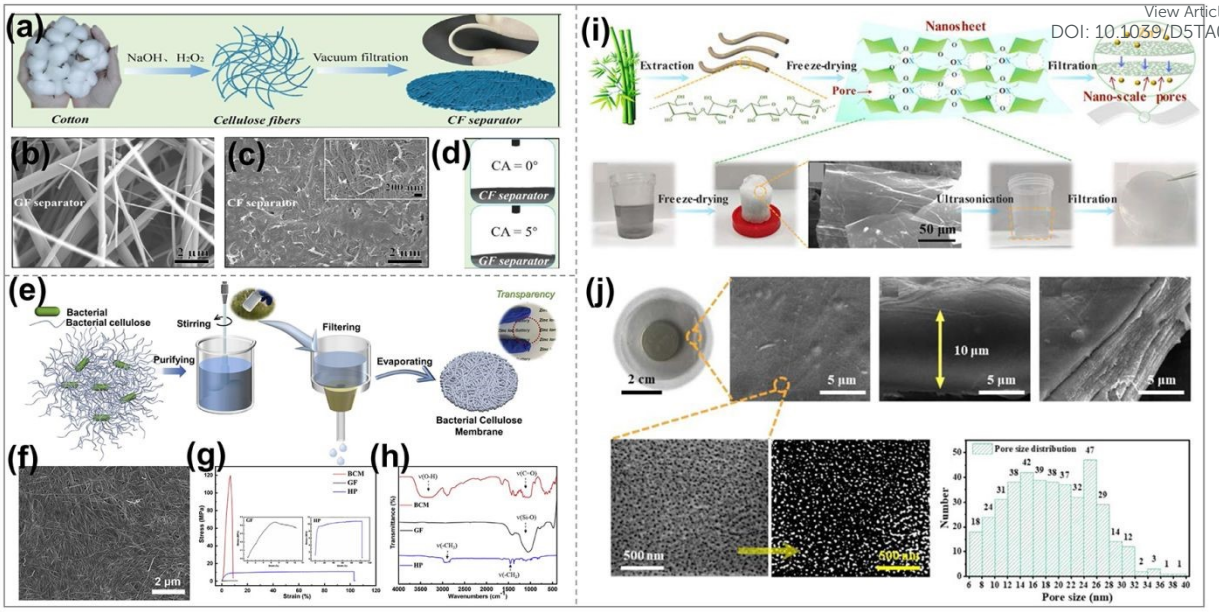

Fig. 3. (a) Schematic illustration of the fabrication process for CF separator. SEM images of (b) GF separator and (c) CF separator. (d) Optical images of the contact angle with 2 M $ZnSO_4$ aqueous electrolyte on the surface of CF and GF separators. Reproduced with permission Ref. [55]. Copyright 2022, Elsevier. (e) Schematic illustration of preparing BCM. (f) SEM image, (g) Tensile curves and (h) FT-IR spectrum of BCM. Reproduced with permission Ref. [28]. Copyright 2022, Elsevier. (i) The preparation process of bamboo cellulose membrane. (j) SEM images and pore size distribution of bamboo cellulose membrane. Reproduced with permission Ref. [56]. Copyright 2022, Elsevier.

assessed using contact angle measurements, yielding a contact angle of 0º (Fig. 3d). This result indicates an exceptionally strong affinity between the separator and the electrolyte, primarily attributed to the presence of abundant surface hydroxyl groups in cellulose.

BC is is another type of high aspect ratio nanocellulose that shares a similar chemical structure with plant cellulose, produced by *Gluconacetobacter xylinus*. With exceptional mechanical properties (Tensile strength of 200-300 MPa, Young's modulus of 15-18 GPa), flexibility, and solution processability, BC emerges as acandidate material for battery separators.[57] Zhang et al.[28] demonstrated an ultra-thin BC separator with a thickness of merely 9μm through vacuum filtration method. The BC separator induces preferential Zn(002) plane deposition through surface hydroxyl-mediated ion regulation and enhance the anti-corrosion properties of Zn anodes, thus effectively inhibiting the growth of Zn dendrites. Furthermore, BC-based separators demonstrate complete biodegradation within 36 days in soil, providing substantial benefits in promoting environmental sustainability. As depicted in Fig. 3e, a uniformly dispersed BC suspension was initially prepared via vigorous mechanical stirring in

View Article Online
DOI: 10.1039/D5TA05279C

an aqueous system. The suspension was then transferred into a vacuum filtration apparatus to fabricate a bacterial cellulose membrane (BCM). SEM characterization in Fig. 3f revealed that the BCM consists of nanofibers with a high aspect ratio, showing the hierarchical porous architecture. As confirmed by tensile characterization in Fig. 3g, the BCM shows superior mechanical performance of 120 MPa compared to other separators. Moreover, Fourier-transform infrared (FT-IR) analysis confirmed the presence of hydrophilic groups, such as O-H and C=O, ensuring its superior hydrophilicity (Fig. 3h).

Besides, Fu et al.[56] developed a biomimetic separator featuring a natural nano-porous structure via the self-assembly of bamboo cellulose nanosheets. The separator demonstrates superior mechanical strength, excellent corrosion resistance, and remarkable stability across a broad pH range. Bamboo-derived cellulose undergoes ultrasonic dispersion, followed by freeze-drying, which facilitates hydrogen-bonding-induced self-assembly into nanosheets. Subsequently, vacuum filtration is employed to fabricate semi-transparent bacterial cellulose membranes from the material, as presented in Fig. 3i. The surface hydroxyl ultra-hydrophilicity enabled rapid water molecules absorption via intermolecular hydrogen-bond interactions. During the drying process of the BCM, water evaporation leads to the contraction of the cellulose network, forming a porous structure within the membrane. The interconnected pore network facilitates uniform Zn^{2+} flux distribution as it passes through, thereby promoting uniform deposition on the Zn anode surface. As shown in Fig. 3j, the upper surface of the BCM exhibits a flat and dense morphology, featuring the abundant nanoscale pore structure with uniformly distributed pores ranging in size from 6 to 32 nm. Ma et al.[58] reported a novel biomass bamboo membrane (BM) separator with oxygen-containing functional groups to suppress water molecule activity. This BM separator incorporates a unique, multi-tiered 2D interlayer that promotes rapid Zn^{2+} diffusion. Moreover, the oxygen functional groups of the BM separator can interact with water molecules through hydrogen bonding, thus achieving outstanding electrochemical performance. Additionally, the stability of Zn anodes can be enhanced by natural cellulose materials, which function either via gelation treatment or as a sandwich structure.[59,60] For example, Wang et al.[61] designed a bilayer separator consisting of commercial butter paper and GF membrane. The dense cellulose-based butter paper exhibited low Zn affinity and high mechanical strength, which effectively prevents Zn dendrites penetration and suppresses dendrite growth. Consequently, the bilayer separators endow Zn||Zn symmetrical batteries with a stable lifespan over 5000 h, highlighting the effectiveness of the bilayer separator in aqueous ZIBs.

Except for cellulose materials, other biomass materials, including chitin, chitosan and lignin,

View Article Online
DOI: 10.1039/D5TA05279C

are also promising candidates for fabricating separators in ZIBs.[62-64] For instance, Wang et al.[29] proposed a simple and scalable strategy for fabricating a chitin nanofiber membrane separator, utilizing chitin extracted from shrimp and crab shells via TEMPO-mediated oxidation to prepare TCh nanofiber suspensions. Afterwards, TCh separators were prepared through a sequence of wet grinding, casting drying, and hot pressing steps (Fig. 4a). These separators are functionalized with zincophilic functional groups (e.g., –COOH, –OH, and –O=C–NH), which synergistically promote Zn^{2+} desolvation process, significantly enhancing the Zn^{2+} transference number. SEM images in Fig. 4b-c indicated that the TCh separators exhibited a densely packed microstructure with nanoscale pores distributed across the surface. The distinctive structural features of the TCh separators facilitate the uniform Zn deposition onto the electrode surface, thereby significantly improving the cycling stability and safety performance of ZIBs. Yang et al.[65] employed chitosan-modified filter paper separators for application in aqueous ZIBs. As illustrated in the Fig. 4d, chitosan was successfully introduced onto the filter paper with the assistance of acetic acid and polyethylene glycol. Subsequently, PEG and other auxiliary agents were thoroughly removed by washing with a NaOH solution. SEM images in Fig. 4e further confirm the formation of a uniform chitosan coating on the surface of filter paper fibers. The hydroxyl, amino, and ether groups within chitosan exhibit preferential adsorption of protons, Zn^{2+}, and sulfate ions, thereby effectively suppressing proton activity and mitigating both corrosion reactions and HER. Notably, the preparation method for the chitosan-modified filter paper separator is simple, cost-effective, and easily scalable, offering a practical and efficient solution for high-performance aqueous ZIBs. Moreover, chitosan can serve as a protective barrier for Zn anodes using a gelation process. For example, Meng et al.[66] developed a polyzwitterionic protective layer by incorporating 2-methacryloyloxyethyl phosphorylcholine into carboxymethyl chitosan (CMCS). The interaction between $ZnSO_4$ and CMCS enhances the interfacial compatibility, thereby significantly improving ion transport. This protective layer not only effectively enhances the stability of Zn anodes under ultra-high current densities, but also extends the cycling lifespan of full cells and hybrid capacitors.

Lignin has also been utilized to prepare separator for ZIBs owing to its abundant functional groups, which help suppress Zn dendrites and enhance Zn^{2+} transport.[67] Recently, Yuan et al.[68] reported a lignin@Nafion composite membrane as separator for ZIBs, which significantly enhanced the cycling performance through increasing water channels and ionic conductivity. Given that lignin is abundant in hydroxyl groups and cost-effective, biomass-derived lignin was introduced to construct additional conductive pathways within the Nafion matrix (Fig. 4f). The incorporation of lignin into Nafion was accomplished via solution casting, allowing for the

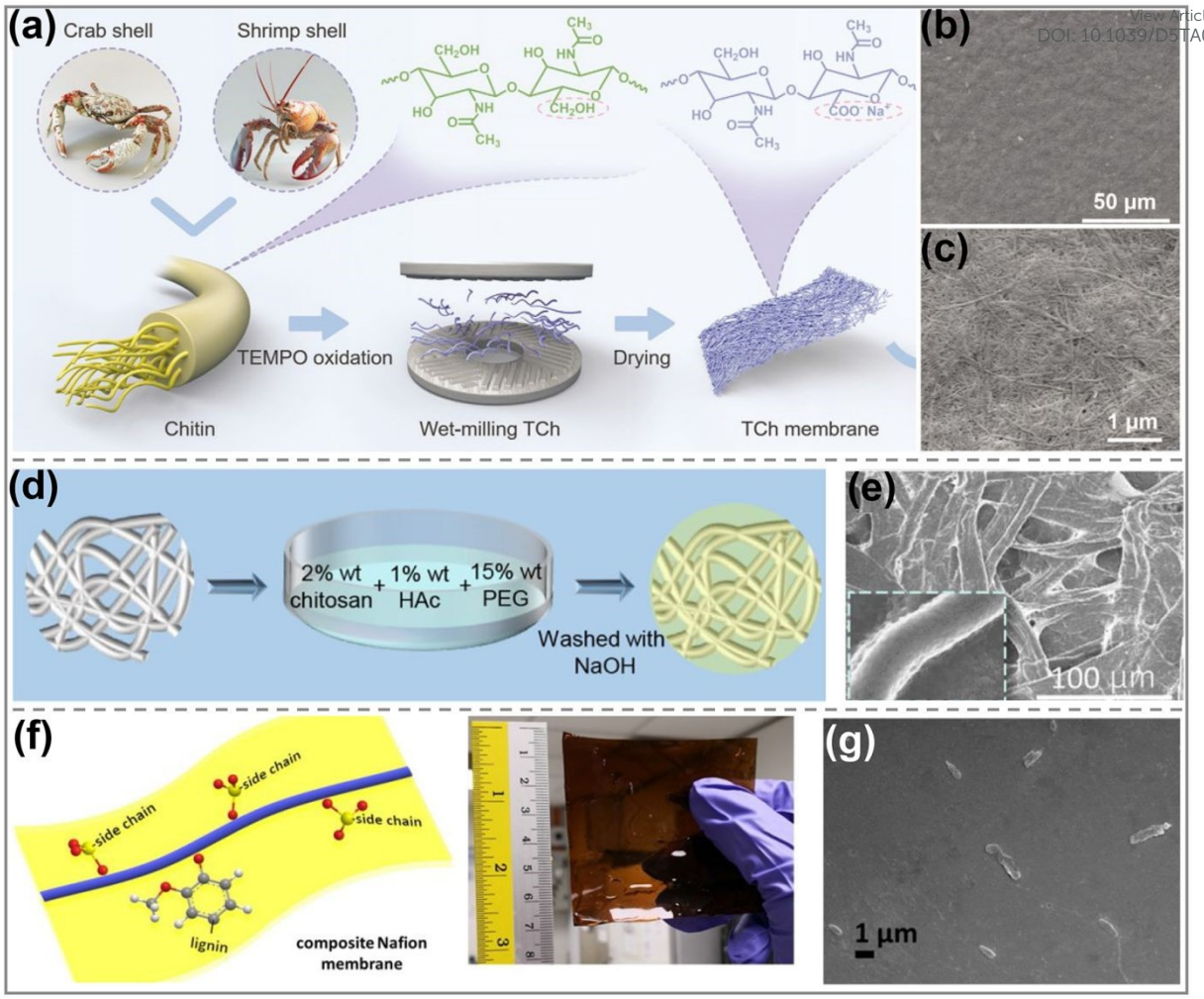

Fig. 4. (a) Schematic illustration of the preparation process for the TCh membrane. (b-c) SEM images of the TCh membrane. Reproduced with permission Ref. [29]. Copyright 2024, Wiley-VCH. (d) Schematic illustration of the preparation process for CS-filter paper. (e) SEM images of CS-filter paper. Reproduced with permission Ref. [65]. Copyright 2022, Elsevier. (f) Scheme illustrating the design of composite biomass waste lignin@Nafion membranes. (g) SEM image of lignin@Nafion membrane. Reproduced with permission Ref. [68]. Copyright 2019, Wiley-VCH.

preparation of composite membranes with varying lignin contents. As depicted in Fig. 4g, lignin was uniformly dispersed within the Nafion matrix, forming slender aggregates that facilitated rapid ion transport. Li et al.[69] prepared a lignocellulose nanofiber (LCNF) separator derived from waste palm, demonstrating dual functionalities of water gating and zinc sieving. The fabrication process of the LCNF separator involves a microwave-assisted deep eutectic solvent (DES) pretreatment, followed by the ultrasonic treatment. By optimizing the type of DES, LCNF with low lignin content (15.5%) and high yield (56.8%) was successfully synthesized. Through its dual functionalities of water gating and zinc sieving, the LCNF separator effectively

View Article Online
DOI: 10.1039/D5TA05279C

regulates the diffusion and transport of Zn^{2+} at the Zn anode/separator interface, thereby enhancing Zn deposition kinetics and mitigating corrosion reactions.

3.1.2 Functional Groups Modified Separator based on Biopolymers

Prominently, the abundant hydroxyl groups in biopolymer backbones offer numerous reactive sites to various chemical modifications and hybridization.[70,71] Therefore, it is an effective strategy to realize the uniform Zn^{2+} flux distribution and rapid Zn^{2+} transport by adjusting surface functional groups to optimize the zinc affinity. Carboxyl, amino, and sulfonate groups are commonly introduced functional groups. Zhang et al.[72] reported that ultra-long cellulose nanofibers (CNF) were synthesized by *aerobic bacteria* using glucose as the carbon source via a biosynthesis process (Fig. 5a). Compared to cellulose nanocrystals or fibers derived from plant sources, this biosynthesized cellulose exhibits superior characteristics, including nearly 100% cellulose content, a high aspect ratio, and enhanced crystallinity. Following TEMPO-mediated oxidation treatment, carboxyl functional groups were successfully incorporated into the cellulose clain. SEM image revealed that the the carbonylation modification cellulose membranes (CCM) consisted of stacked and interwoven ultra-long nanofibers (Fig. 5b). The carboxyl-functionalization endowed the CCM separator with rapid Zn^{2+} transpor, thereby effectively suppressing Zn dendrite growth and prolonging the cycle life of aqueous ZIBs. In addition, biomass materials sourced from fibers, like viscose fibers and cellulose esters, could also potentially be effective separator candidates for zinc-ion batteries.[73,74] Recently, Ou et al.[73] presented a cost-effective commercial viscose fabric as a separator for aqueous ZIBs. This separator, consisting of viscose fibers with surface grooves and abundant carboxyl groups, facilitates epitaxial pathways for Zn^{2+} via its surface grooves. Through its surface grooves and carboxyl groups, the viscose fiber separator can facilitate the desolvation of hydrated Zn^{2+} to suppress HER. Consequently, this separator not only enhances the cycling stability of ZIBs but also offers a low-cost material solution.

Furthermore, sulfonate functional groups have emerged as promising modifiers for biomass-based separators due to their strong hydrophilicity and ion-exchange capability. These negatively charged moieties induce charge screening effects that effectively homogenize Zn^{2+} flux distribution and inhibit the migration of SO_4^{2-} ions. For instance, Yan et al.[75] fabricated the independent and rollable sulfonated bacterial cellulose (SBC) separators via the sequential processes of sulfonation, washing, and dehydration (Fig. 5c-d). During this process, the negatively charged $-SO_3^-$ groups were introduced by substituting a portion of the primary hydroxyl groups on the cellulose chains. The resultant SBC separators maintained an ordered three-dimensional nanofiber network structure similar to that of the original BC separators,

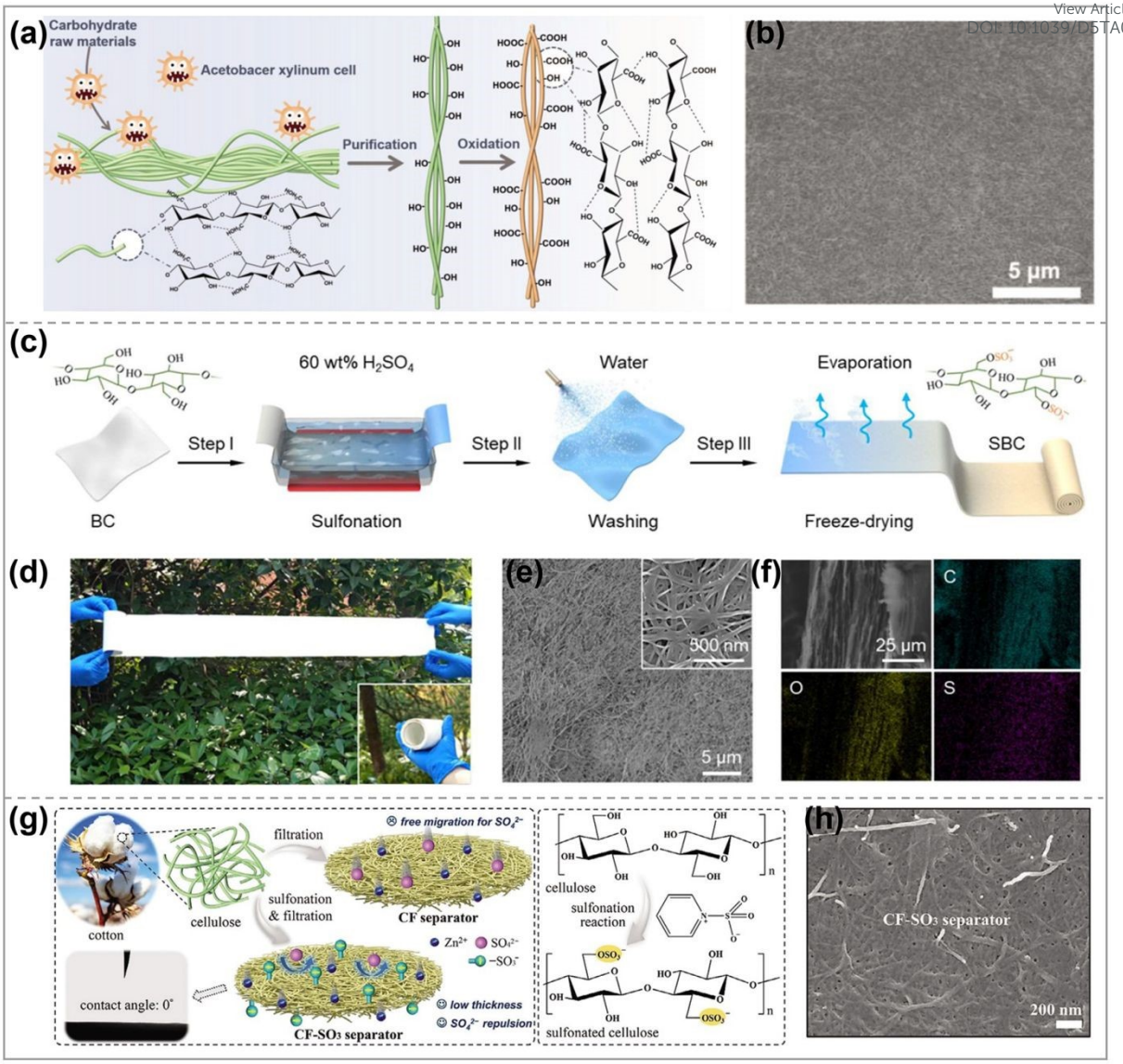

Fig. 5. (a) Schematic illustration of the preparation process for bio-synthesized cellulose nanofibers and modification. (b) SEM image of CCM. Reproduced with permission Ref. [72]. Copyright 2023, Wiley-VCH. (c) Schematic illustration of scalable production for SBC separators. (d) Photographs of the rolled separator. SEM images of (e) surface and (f) cross-section of SBC separators. Reproduced with permission Ref. [75]. Copyright 2025, Elsevier. (g) Schematic illustration of the preparation processes and the sulfonation modification on cellulose. (h) SEM image of CF-SO_3 separator. Reproduced with permission Ref. [76]. Copyright 2024, Wiley-VCH.

thereby exhibiting superior high porosity (Fig. 5e-f). More impressingly, the $–SO_3^-$ groups within the SBC separators effectively suppressed the migration of SO_4^{2-} ions and facilitated the rapid Zn^{2+} transport, thus enabling uniform Zn^{2+} flux and dendrite-free Zn deposition behavior. Besides, cellulose fiberse extracted from agricultural cotton were also employed for preparation of sulfonated cellulose separator (CF-SO_3) through a sulfonation reaction (Fig. 5g).[76] Owing to

View Article Online
DOI: 10.1039/D5TA05279C

electrostatic interactions, the CF-SO_3 membranes effectively suppress the migration of SO_4^{2-} ions, achieving superior ion sieving performance. SEM image revealed that the CF-SO_3 membranes possess uniformly distributed nanopore structures (Fig. 5h). This separator significantly improved the cycling stability and Zn deposition behavior, thereby effectively inhibiting the formation of Zn dendrites. Zhang et al.[77] reported a Janus separator by growing sulfonated cellulose-modified graphene sheets on one side of a commercial GF separator via spin-coating. Due to the presence of sulfonate groups, the composite separator can spontaneously repel SO_4^{2-} ions and anchor H^+ species, promoting efficient Zn^{2+} transport and minimizing side reactions. Ge et al.[33] successfully developed a single-ion functionalized nanocellulose membrane (CNF-SO_3Zn) by replacing Na^+ ions in CNF-SO_3Na with Zn^{2+} via ion exchange technology, thereby enabling preferential conduction of Zn^{2+} (Fig. 6a). Given that sulfonate anions are chemically anchored to the cellulose chains, Zn^{2+} ions theoretically serve as the primary mobile charge carriers and migrate within the CNF-SO_3Zn membrane under an applied electric field. TEM image revealed that CNF-SO_3Zn membrane exhibits a high aspect ratio and large specific surface area, which contributes to the superior mechanical properties (Fig. 6b). Notably, CNF-SO_3Zn membrane can be manufactured at an industrial scale using conventional papermaking techniques (Fig. 6c).

Through surface amine functionalization, Zhang et al.[44] successfully converted natural nanocellulose (a-NCFs) into cationic nanocellulose (c-NCFs). This functionalization strategy not only introduced cationic groups but also preserved the hierarchical mesoporous structure of nanocellulose, thereby enabling its intrinsic ion sieving capability. Specifically, nanocellulose derived from green algae was chemically modified via an epichlorohydrin-trimethylamine chloride condensation reaction to fabricate cationically charged nanocellulose materials (Fig. 6d). The introduced cationic amine groups interact with SO_4^{2-} ions and repel desolvated Zn^{2+} through electrostatic interactions, which enhances the concentration and uniformity of Zn^{2+} flux within the pores of the nanocellulose separator. SEM images revealed that these two separators exhibit a mesoporous structure composed of entangled nanofibers with diameters of approximately 20 nm (Fig. 6e-f). Furthermore, the c-NCFs separator demonstrated excellent mechanical flexibility and bendability (Fig. 6g). The experiment result showed that the cationic amine groups immobilized on the NCFs can improve the Zn^{2+} transference number and eliminate the “tip effect” through electrostatic shielding.

The development of separators using two types of biomass materials showcases a sustainable approach for ZIBs.[78] These biomass-based separators exhibit superior mechanical strength and ionic conductivity, facilitating efficient Zn^{2+} transport while minimizing environmental impact.

View Article Online
DOI: 10.1039/D5TA05279C

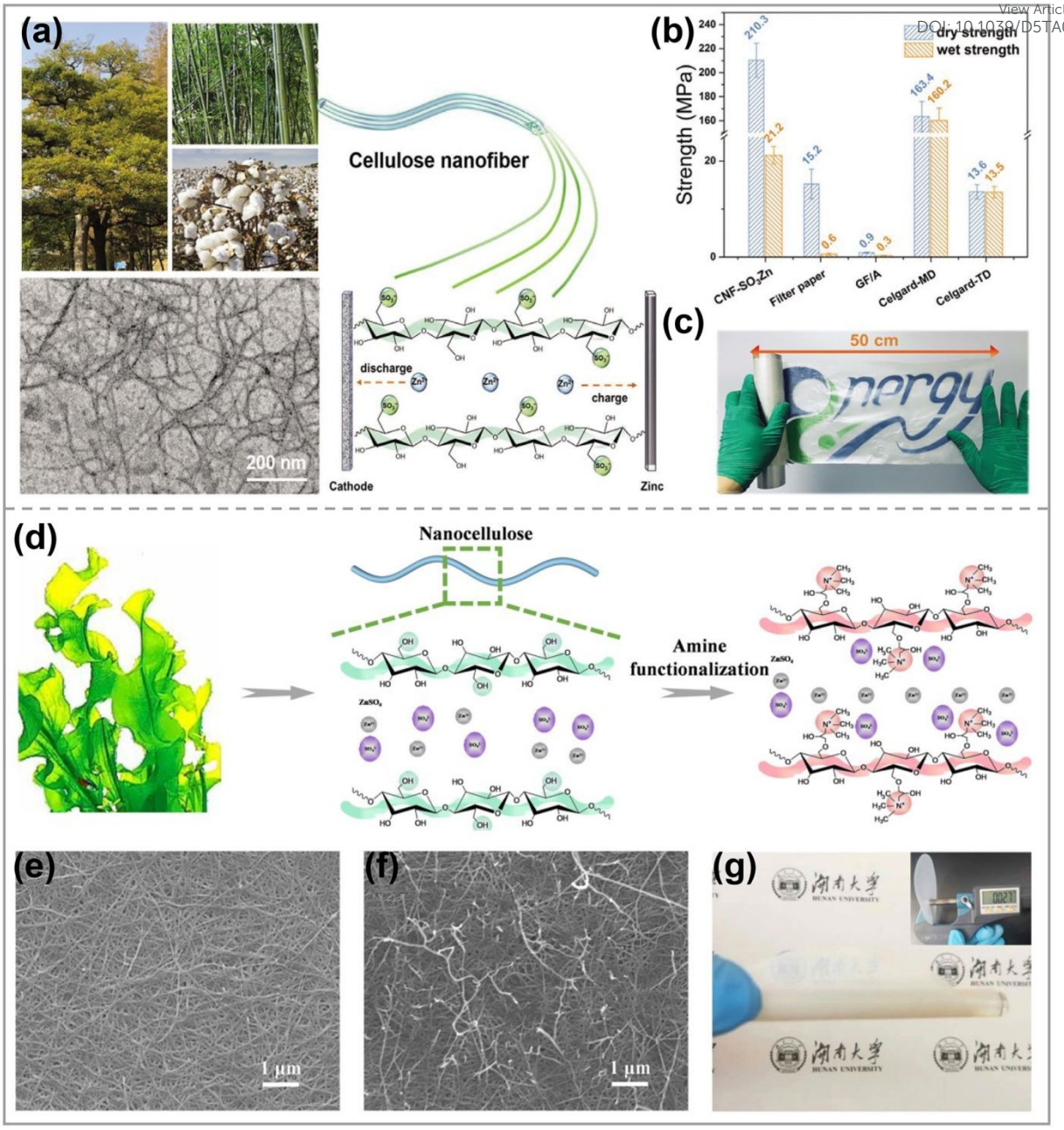

Fig. 6. (a) Schematic illustration of the preparation process for the CNF-SO_3Zn membrane. (b) The dry strengths and wet strengths of different membranes. (c) A digital photo image of an as-synthesized CNF-SO_3Zn membrane. Reproduced with permission Ref. [33]. Copyright 2022, Wiley-VCH. (a) Schematic illustration of the preparation process for c-NCFs separators. SEM images of a-NCFs separator (b) and c-NCFs separator (c). (d) The digital image of c-NCFs separator. Reproduced with permission Ref. [44]. Copyright 2023, Elsevier.

Recently, Ma et al.[50] developed an anisotropic and biodegradable separator using nanofibrillated cellulose (NFC) and chitosan (V-NFC-CS) for ZIBs, inspired by the hierarchical structure of wood. Based on the directional freezing technology, the V-NFC-CS separator exhibited a high modulus and facilitate efficient Zn^{2+} transport channels in the vertical direction.

Typically, an aqueous dispersion of NFC and chitosan was poured onto a copper ingot with the lower half immersed in liquid nitrogen for directional freezing. Subsequently, freeze-drying and compression treatments were applied, yielding a separator with vertically aligned channels (Fig. 7a). Clearly, the V-NFC-CS separator exhibited uniformly distributed and parallel channels in the *xz* plane, while numerous pores were observed in the *xy* plane (Fig. 7b). As shown in Fig. 7c-d, the average Derjaguin-Muller-Toporov (DMT) modulus of the V-NFC-CS separator was 7.3 GPa, which is approximately 3.3 times higher than that of the NFC-CS separator (2.2 GPa). The theoretical calculations and experimental results demonstrate that the V-NFC-CS separator can efficiently inhibit the vertical deposition of Zn, leading to a dendrite-free structure and reduced parasitic reactions. Furthermore, a cellulose-derived biomass

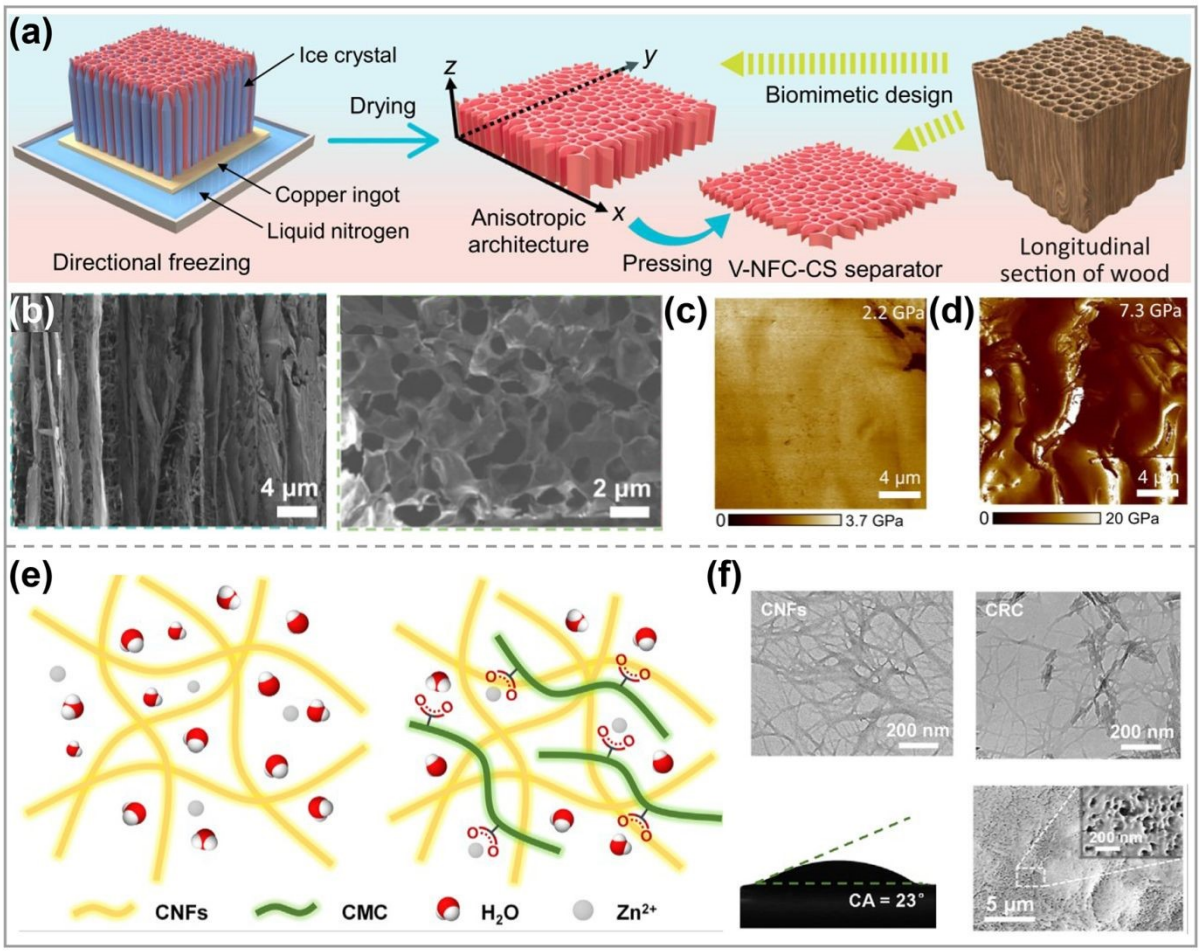

Fig. 7. (a) Schematic illustration of the preparation process for V-NFC-CS separator. (b) SEM images of V-NFC-CS separator. DMT modulus distributions of (c) NFC-CS separator and (d) V-NFC-CS separator. Reproduced with permission Ref. [50]. Copyright 2025, Springer Nature. (e) Schematic illustration of the preparation process for CNF and CRC separators. (f) TEM images of CNF and CRC, contact angle and SEM images of CRC separator. Reproduced with permission Ref. [43]. Copyright 2024, Elsevier.

View Article Online
DOI: 10.1039/D5TA05279C

separator (CRC) was developed using a straightforward sol-gel preparation method. This CRC separator consists of carboxymethyl cellulose (CMC) and CNF, in which CNF was utilized as the structural matrix and CMC was introduced as the optimizing component (Fig. 7c). As a result, the overall production cost was significantly reduced, while the biodegradability of the CRC separator was enhanced. The distribution and interaction of the two cellulose components within the CRC separator were clearly visualized in the TEM images (Fig. 7f). Besides, the contact angle measurement of the CRC separator confirm its excellent hydrophilic properties. The results indicated that the hydrogen bond cross-linking between two cellulose components enhanced the mechanical strength of the CRC separator to inhibit dendrite growth, and the zincophilic functional groups improved Zn^{2+} binding, promoting uniform Zn nucleation and deposition.

On the basis of the above-mentioned relative literatures, pure biomass separators offer significant several advantages owing to their sustainability and environmental friendliness derived from natural sources: 1) the abundant functional groups (e.g., hydroxyl, carboxyl, sulfonate, and amino groups) facilitate the regulation of ion transport, promote uniform Zn deposition, and capture free water molecules to suppress water-induced corrosion; 2) the distinctive porous network structure of biomass materials improves electrolyte wettability and ion diffusion balance; 3) the inherent biodegradability of pure biomass separators provides substantial benefits for the environmentally conscious design of ZIBs. Nevertheless, several limitations still remain: 1) insufficient mechanical strength increases the risk of structural failure under repeated cycling; 2) heterogeneous pore distribution induced by variations in crystallinity may accelerate Zn dendrite formation. Therefore, the enhancement of overall performance through composite modification and microstructure engineering, while retaining the inherent characteristics of biomass materials, presents a significant challenge in current research efforts.

3.2 Biomass-based Composite Separators

To further improve the performance of the biomass-based separator, biomass materials are frequently combined with organic or inorganic materials to fabricate composite separators. This hybrid design can significantly improve the pore structure and zinc affinity of the biomass-based separator, thereby achieving a homogeneous Zn^{2+} flux distribution and uniform Zn deposition.[38,79-82] For example, Yang et al.[39] constructed nitrogen-modified graphdiyne (NGDY) interface on cellulose separator (CS@NGDY) for ZIBs via a triazine monomer-based triethynyl cross-coupling reaction, in which the chlorin atoms in cyanuric chloride were substituted with acetenyl groups (Fig. 8a). The NGDY interface can regulate the pH at the Zn anode interface,

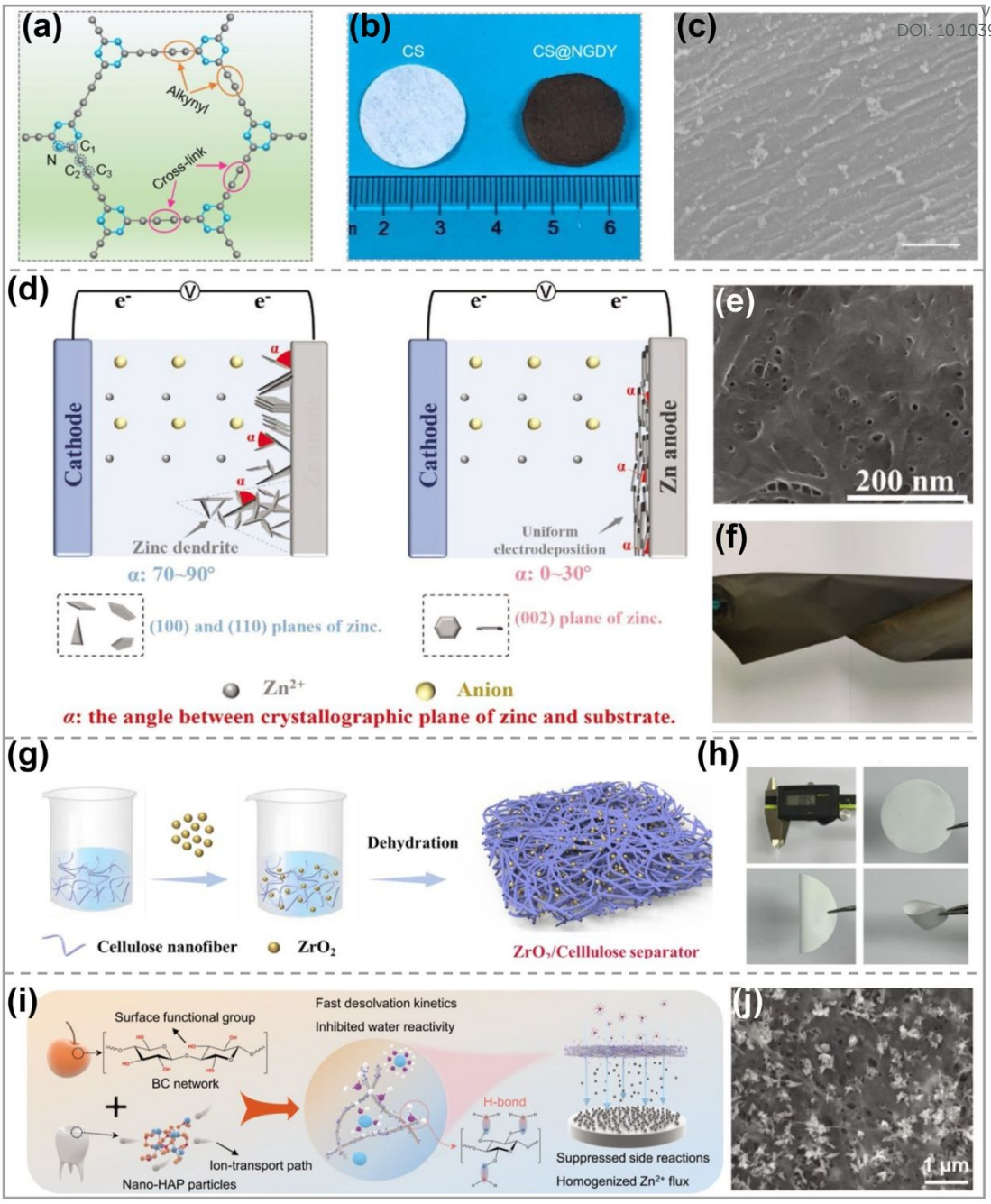

Fig. 8. (a) The chemical structure of NGDY. (b) Digital image and (c) Raman spectra of CS@NGDY separator. Reproduced with permission Ref. [39]. Copyright 2022, Wiley-VCH. (d) Schematic illustration of Zn^{2+} deposition with (100) or (110) planes and (002) plane as dominant. (e) SEM image of CG separator. (f) Optical photograph of CG separator. Reproduced with permission Ref. [40]. Copyright 2021, Wiley-VCH. (g) Schematic illustration of the preparation process for ZC separator. (h) Thickness and flexibility measurement of ZC separator. Reproduced with permission Ref. [41]. Copyright 2021, Elsevier. (i) Schematic illustration of the preparation process for the nature-inspired ZnHAP/BC separator and its effect in regulating Zn deposition behavior. (j) SEM image of ZnHAP/BC separator. Reproduced with permission Ref. [83]. Copyright 2023, Wiley-VCH.

View Article Online
DOI: 10.1039/D5TA05279C

thereby improving the cycling stability and rate performance. As shown in Fig. 8b, it can be observed that the cellulose separator changed color from white to dark brown upon the incorporation of NGDY. Furthermore, SEM image demonstrated that the cellulose separator was effectively encapsulated by NGDY through its 2D nanosheet structure (Fig. 8c). The NGDY interface plays a crucial role in significantly decreasing the activation energy for the desolvation of hydrated Zn^{2+}, thereby stabilizing the interfacial pH and inhibiting Zn dendrite formation. Cao et al.[40] reported a functional separator composed of cellulose nanofibers and graphene oxide (CG) using the solution casting method. The CG separator exhibited a negative surface charge and contains abundant oxygen-containing functional groups with high Zn affinity, which facilitates strong interactions with Zn^{2+} and guides Zn deposition along the (002) crystal plane (Fig. 8d). SEM images revealed that the CG separator possesses numerous pores with diameters ranging from 10 to 50 nm (Fig. 8e). Moreover, Fig. 8f demonstrated that the CG separator maintains a smooth surface even after dehydration and retains excellent flexibility after being bent at various angles. Therefore, these characteristics suggest that the CG separator holds great promise for application in flexible ZIBs. Luo et al.[82] developed a graphene oxide-modified cellulose acetate separator via a simple and cost-effective filtration method. The composite separator features low lattice mismatch and numerous hydrophilic oxygen-containing functional groups, which effectively facilitate the epitaxial electro-deposition of Zn, leading to a dendrite-free Zn metal surface.

In recent years, a series of inorganic materials incorporated into cellulose separators have been widely studied for ZIBs to achieve synergistic enhancement in ionic conductivity and mechanical strength through interface engineering. These materials include zirconium dioxide,[41,84] lithium magnesium silicate,[79] strontium titanate,[85] tungsten carbide,[86] titanium nitride,[87] halloysite nanotubes,[88] MXene,[89] boron nitride,[90] and etc. Qin and co-workers[41] fabricated a cellulose nanofibers-ZrO_2 composite (ZC) separator for ZIBs via a facile and cost-effective solution casting method (Fig. 8g). Owing to the superior dielectric properties of ZrO_2 particles, the ZC separator can induce Maxwell-Wagner polarization under an external electric field. This characteristic not only facilitates the uniform Zn deposition but also enhances the diffusion kinetics of Zn^{2+} while effectively repelling anions, thereby significantly improving the stability of the Zn anode and inhibiting side reactions. Moreover, the experimental results demonstrate that the ZC separator exhibits superior mechanical stability and electrochemical performance even under bending or folding conditions (Fig. 8h), thus providing strong evidence for its potential application in flexible ZIBs. Then, the research group[91] developed a multifunctional composite separator based on industrial waste fly ash particles and cellulose

View Article Online
DOI: 10.1039/D5TA05279C

nanofibers (FACNF) for ZIBs. The FACNF separator exhibted high ionic conductivity and a low desolvation energy barrier, whihc effectively directs the epitaxial electrodeposition of Zn, thereby achieving superior Coulombic efficiency and cycling stability. Qin et al.[83] reported a novel biomimetic separator (ZnHAP/BC) by integrating BC with nano-hydroxyapatite (HAP) particles. Typically, this advanced separator comprises an interwoven BC fiber network decorated with nano-HAP particles, which was formed through hydrogen-bond self-assembly. Subsequently, the as-prepared ZnHAP/BC separator underwent ion-exchange treatment in a $ZnSO_4$ solution to incorporate Zn^{2+} into the HAP structure (Fig. 8i). SEM images in Fig. 8j revealed that ZnHAP particles are uniformly anchored within the interwoven BC nanofiber network. Therefore, this ZnHAP/BC separator not only suppressed water activity via surface functional groups to mitigate water-induced side reactions, but also enhanced Zn^{2+} transport kinetics and homogenizes Zn^{2+} flux, enabling rapid and uniform Zn deposition. Recently, Ma et al.[92] developed a lignocellulose-based membrane modified with an amino-functionalized metal-organic framework (UiO-66-NH_2) for ZIBs. This composite membrane (LC@UiO-66-NH_2) was fabricated via a simple vacuum filtration process. The as-prepared LC@UiO-66-NH_2 separator featured a low thickness (20μm), high mechanical strength (47.4 Mpa), excellent flexibility, good hydrophilicity, and a high ionic conductivity (17.2 mS/cm). Notably, the amino functional groups demonstrated strong affinity toward Zn^{2+} and form robust hydrogen bonds with water molecules, thereby facilitating the uniform Zn deposition and efficient transport of Zn^{2+}.

Generally speaking, biomass-based composite separators composed of biomass and inorganic materials demonstrate several synergistic advantages: First, the incorporation of inorganic components significantly enhance mechanical strength and thermal stability, effectively addressing the structural fragility of pure biomass separators; Second, the designed hierarchical architectures combining biomass porous networks with inorganic components enables the formation of dual-path ion regulation mechanisms, simultaneously suppressing dendrite growth and improving ionic conductivity. Finally, inorganic fillers with catalytic activity may mitigate electrode passivation and reduce interfacial side reactions. Despite these advantages, the interfacial incompatibility between organic and inorganic phases often causes delamination during cycling, the limitations in mass loading of active components can compromise flexibility, and the complex manufacturing processes raise concerns regarding cost-effectiveness and scalability.

3.3 Coated Modified Biomass-based Separators

To further enhance the stability of the Zn anode, a biomass separator can be served as the

View Article Online
DOI: 10.1039/D5TA05279C

substrate, and then coated inorganic or organic materials on the one side, thereby effectively optimizing the Zn deposition interface.[93-98] These coatings can improve ionic conductivity and reduce interfacial resistance, facilitating efficient Zn^{2+} transport. Moreover, they provide structural stability and mitigate Zn dendrite growth, thereby promoting the overall safety and lifespan of ZIBs. For example, Zheng et al.[42] reported a Janus separator (AgNWs/BC) consisting of a bacterial cellulose (BC) layer on one side and a silver nanowire/bacterial cellulosecomposite layer on the other side (Fig. 9a). As depicted in Fig. 9b, the AgNWs/BC membrane exhibited a uniform silver-gray color, in sharp contrast to the white appearance of the pure BC membrane. It can be observed that the BC nanofibers were intricately intertwined to form a dense nanostructure, abd the well-defined bilayer structure of the Janus separator revealed a markedly enhanced silver signal in the upper layer. Furthermore, the halo-ring pattern confirms that the silver nanowires are tightly encapsulated by bacterial cellulose, forming a robust interfacial layer. Owing to the high Zn affinity and excellent electrical/thermal conductivities of silver nanowires, the as-prepared AgNWs/BC separator acts as an ion pump to accelerate Zn^{2+} transport kinetics in the electrolyte. As a consequence, the AgNWs/BC separator enabled rapid and uniform Zn deposition while effectively suppressing Zn dendrite formation. Hou et al.[99] employed a direct-current magnetron sputtering system to deposit a Sn layer onto a cellulose separator with a thickness of 30 μm. This Sn coating can effectively regulate the electric field distribution, thereby facilitating the smooth and uniform Zn deposition while inhibiting the formation of Zn dendrites. Moreover, the high Zn affinity of the Sn coating enabled the preferential deposition of Zn^{2+} on its surface, leading to a "face-to-face" growth mode that suppresses Zn dendrite formation and greatly enhances the cycling stability (Fig. 9c). The optical and SEM images in Fig. 9d-e indicated that a uniform gray Sn coating was formed on the white separator surface after sputtering treatment, and the surface of Sn-coated separator was uniformly covered with Sn nanoparticles with an average diameter of around 60 nm. The results indicate that the Sn-coated separator demonstrates excellent electrical conductivity and strong Zn affinity, effectively modulating the Zn deposition behavior and enhancing the cycling stability of ZIBs. Li et al.[100] developed a functional ultra-thin separator (FCNF) with a thickness of 23 μm to modulate the zinc deposition interfacial chemistry. This FCNF separator consists of a CNF membrane matrix with excellent mechanical strength and a uniform nano-porous structure, as well as a C/Cu nanocomposite modified layer enriched with Zn-binding sites (Fig. 9f). The C/Cu nanocomposite material was synthesized via the pyrolysis of Cu-MOF precursors, featuring a high specific surface area along with small-sized Cu nanoparticles. These properties effectively mitigate local current density, promote uniform zinc nucleation, and significantly

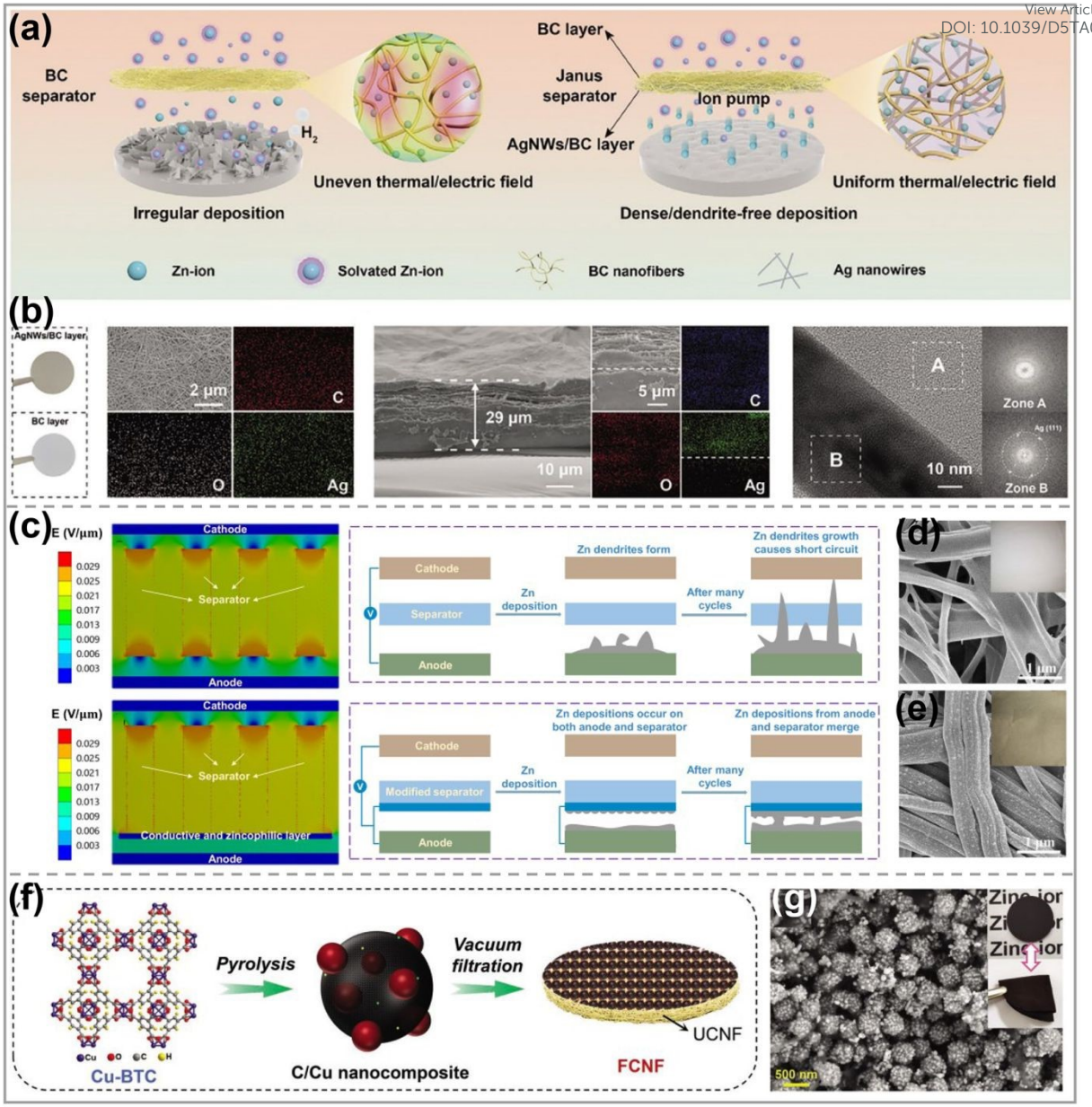

Fig. 9. (a) Schematic illustration of the preparation process for Janus separators. (b) Optical photos, SEM images, and HRTEM images of Janus separator. Reproduced with permission Ref. [42]. Copyright 2023, Wiley-VCH. (c) Electric field distribution and schematic illustration of Zn deposition with the pristine separator and Sn-coated separator. (d) the pristine separator and (e) Sn-coated separator with the corresponding optical photos in the insets. Reproduced with permission Ref. [99]. Copyright 2021, Springer Nature. (f) Schematic illustration and (g) top-view SEM image of the FCNF separator. Reproduced with permission Ref. [100]. Copyright 2023, Wiley-VCH.

enhance Zn deposition kinetics. Furthermore, the surface modification layer with approximately 3 μm in thickness was composed of numerous quasi-spherical C/Cu nano-composite particles. The surface modification layer demonstrated excellent flexibility, which

View Article Online
DOI: 10.1039/D5TA05279C

allows it to be folded and wound together with the UCNF matrix (Fig. 9g). Recently, Zhang et al.[101] reported a bifunctional cellulose nanocrystal whisker-graphene (CNG) membrane for ZIBs.This CNG membrane functions as a desolvation layer to prevent water molecules from reaching the Zn anode, thereby mitigating the water-induced corrosion reaction. Besides, the CNG membrane exhibited a negative surface charge that induces a deionization effect, which repels anions and guides cations for the directional deposition of Zn parallel to the (0002) Zn plane. The CNG membrane demonstrated superior flexibility and mechanical strength, enabling it to withstand tensile and puncture forces while adapting to the surface fluctuations of the Zn anode during the plating/stripping process.

Coated modified biomass-based separators have emerged as a promising strategy to address critical challenges in aqueous ZIBs, offering several advantages including improved ionic conductivity, enhanced mechanical stability, and reduced interfacial resistance.[102-104] The hierarchical porous structure of biomass substrates (e.g., cellulose) ensures efficient electrolyte penetration and mechanical flexibility, and the single-sided functional coating permits directional regulation of Zn^{2+} flux, effectively guiding Zn deposition toward the coated surface. This asymmetric design maintains inherent biodegradability of biomass and introduces interfacial modification capabilities. In addition, various materials, including conductive polymers and carbon-based materials, are suitable for coating modification, which can further improve the performance of separators in ZIBs. However, significant challenges remain in achieving large-scale production without compromising performance. Interfacial incompatibility between organic/inorganic phases often induces delamination during long-term cycling, and coating thickness uniformity remains technically challenging, particularly for large-area manufacturing. Future research should focus on 1) developing low-cost roll-to-roll coating technique to ensure uniformity; 2) designing self-healing coatings to mitigate mechanical stress; 3) optimizing hybrid coatings with dual functionalities.

4. Operational Mechanism of Biomass-based Separators

Zn anode suffers significant challenges attributed to the uncontrollable growth of Zn dendrites and undesirable side reactions. As a critical component, the separator plays an indispensable role in mitigating these challenges by functioning as a physical barrier and a regulator of the chemical environment. Biomass-based separators have garnered considerable attention due to their distinctive microstructures and diverse functional groups. For example, biomass-based separators can guide Zn deposition to preferentially occur along the (002) crystal plane via specific surface characteristics, effectively suppressing Zn dendrite formation. Furthermore, the

View Article Online
DOI: 10.1039/D5TA05279C

Table 1. Summary of the electrochemical performances of ZIBs using various biomass-based separators.

Separator	Ionic conductivity (mS cm^{-1})	Zn^{2+} transference number	Current density/areal capacity	Overpotential (mV)	Lifespan	Ref.
CF	56.95	0.48	1 mA cm^{-2}/1 mAh cm^{-2} 2 mA cm^{-2}/4 mAh cm^{-2}	50 70	2000 h 850 h	55
BCM	0.61	0.32	0.5 mA cm^{-2}/0.1 mAh cm^{-2} 2 mA cm^{-2}/1 mAh cm^{-2}	54 60	4000 h 450 h	28
Bamboo cellulose membrane	/	/	0.5 mA cm^{-2}/0.25 mAh cm^{-2}	58	5000 h	56
Bamboo membrane	/	0.49	1 mA cm^{-2}/1 mAh cm^{-2} 10 mA cm^{-2}/10 mAh cm^{-2} 30 mA cm^{-2}/30 mAh cm^{-2}	50 90 480	1000 h 325 h 90 h	58
TCh membrane	9.46	0.49	1 mA cm^{-2}/1 mAh cm^{-2} 10 mA cm^{-2}/10 mAh cm^{-2}	50 75	2700 h 320 h	29
CS-filter paper	/	0.62	0.5 mA cm^{-2}/0.5 mAh cm^{-2} 5 mA cm^{-2}/1 mAh cm^{-2}	100 150	2800 h 450 h	65
Lignin-rich microfibrillated cellulose	7.03	/	0.5 mA cm^{-2}/0.5 mAh cm^{-2}	40	200 h	67
Lignin@Nafion membranes	/	/	0.2 mA cm^{-2}/0.2 mAh cm^{-2} 0.6 mA cm^{-2}/0.6 mAh cm^{-2}	41 70	/	68
LCNF	18.10	0.71	0.5 mA cm^{-2}/1 mAh cm^{-2} 8 mA cm^{-2}/8 mAh cm^{-2}	60 85	3500 h 300 h	69
CCM	1.04	/	1 mA cm^{-2}/1 mAh cm^{-2} 5 mA cm^{-2}/1 mAh cm^{-2}	45 62	2800 h 600 h	72
Viscose fabric	5.44	0.61	1 mA cm^{-2}/1 mAh cm^{-2} 2 mA cm^{-2}/4 mAh cm^{-2} 4 mA cm^{-2}/4 mAh cm^{-2}	95 105 120	4600 h 1180 h 620 h	73
SBC	13.10	/	1 mA cm^{-2}/1 mAh cm^{-2} 5 mA cm^{-2}/10 mAh cm^{-2}	70 80	1170 h 600 h	75
CF-SO_3	52.10	0.60	1 mA cm^{-2}/1 mAh cm^{-2} 2 mA cm^{-2}/4 mAh cm^{-2}	60 80	2500 h 1200 h	76
CNF-SO_3Zn	0.05	0.70	1 mA cm^{-2}/0.5 mAh cm^{-2}	25	100 h	33

View Article Online
DOI: 10.1039/D5TA05279C

c-NCFs	4.83	0.73	1 mA cm^{-2}/4 mAh cm^{-2} 8 mA cm^{-2}/4 mAh cm^{-2} 20 mA cm^{-2}/10 mAh cm^{-2}	40 60 100	1924 h 510 h 180 h	44
Zr-CNF	4.47	0.45	1 mA cm^{-2}/1 mAh cm^{-2} 5 mA cm^{-2}/5 mAh cm^{-2} 10 mA cm^{-2}/2 mAh cm^{-2}	45 50 100	1650 h 660 h 700 h	38
CTNF	3.10	0.62	0.5 mA cm^{-2}/0.5 mAh cm^{-2} 1 mA cm^{-2}/1 mAh cm^{-2} 5 mA cm^{-2}/5 mAh cm^{-2}	42 50 65	1800 h 1450 h 500 h	78
V-NFC-CS	11.80	0.67	10 mA cm^{-2}/2 mAh cm^{-2}	80	100 h	50
CRC	0.13	/	0.5 mA cm^{-2}/0.5 mAh cm^{-2}	50	800 h	43
CS@NGDY	7.39	/	3 mA cm^{-2}/1 mAh cm^{-2} 5 mA cm^{-2}/1 mAh cm^{-2} 10 mA cm^{-2}/1 mAh cm^{-2}	48 75 90	600 h 500 h 200 h	39
Cellulose-graphene oxide	1.99	/	0.5 mA cm^{-2}/0.25 mAh cm^{-2} 2 mA cm^{-2}/1 mAh cm^{-2} 5 mA cm^{-2}/2.5 mAh cm^{-2} 20 mA cm^{-2}/10 mAh cm^{-2}	22 30 55 105	1750 h 1750 h 500 h 400 h	40
Cellulose/ZrO_2	4.59	/	0.5 mA cm^{-2}/0.25 mAh cm^{-2} 5 mA cm^{-2}/2.5 mAh cm^{-2}	57 66	2000 h 1000 h	41
CNF/lithium magnesium silicate	29.30	/	1 mA cm^{-2}/0.5 mAh cm^{-2} 5 mA cm^{-2}/2.5 mAh cm^{-2}	50 85	1000 h 500 h	79
ZnHAP/BC	4.10	0.83	1 mA cm^{-2}/1 mAh cm^{-2}	50	1600 h	83
FACNF	5.76	0.77	2 mA cm^{-2}/1 mAh cm^{-2} 5 mA cm^{-2}/2.5 mAh cm^{-2}	100 125	1650 h 600 h	91
LC@UiO-66-NH_2	17.20	0.73	2 mA cm^{-2}/2 mAh cm^{-2}	70	2000 h	92
AgNWs/BC	3.83	/	2 mA cm^{-2}/1 mAh cm^{-2} 10 mA cm^{-2}/1 mAh cm^{-2} 80 mA cm^{-2}/1 mAh cm^{-2}	50 150 200	2400 h 600 h 1000 h	42
C/Cu@UCNF	/	0.49	1 mA cm^{-2}/0.5 mAh cm^{-2} 5 mA cm^{-2}/2.5 mAh cm^{-2} 10 mA cm^{-2}/2 mAh cm^{-2}	40 50 100	2000 h 650 h 600 h	100
CNG	29.20	/	0.25 mA cm^{-2}/0.5 mAh cm^{-2} 1 mA cm^{-2}/0.5 mAh cm^{-2}	15 21	5500 h 2956 h	101

View Article Online
DOI: 10.1039/D5TA05279C

functional groups in the biomass-based separators can interact with the electrolyte ions to optimize the solvation structure of Zn^{2+}, thereby reducing the activity of free water and inhibiting HER and other side reactions. More impartantly, biomass-based separators can enhance battery performance through multiple synergistic mechanisms, including the prevention of dendrite penetration via high mechanical strength, the promotion of uniform ion flux and electric field distribution, the facilitation of uniform Zn nucleation, and the regulation of pH at the electrode/electrolyte interface to improve chemical stability.

4.1 Regulation of the Crystallographic Orientation during Zn Deposition

Biomass-based separators demonstrate significant potential in optimizing Zn deposition along the (002) crystal plane. Firstly, the enhancement of their zincophilic properties can accomplished by regulating surface functional groups, thereby effectively promoting uniform Zn deposition. Secondly, the physicochemical characteristics of composite materials or coatings can be utilized to further control over Zn deposition behavior. Zhang et al.[28] proposed a distinctive mechanism that the BCM separator regulates Zn deposition behavior. XRD analysis demonstrated that the diffraction intensity of the (002) crystal plane gradually increased during Zn deposition with the BCM separator (Fig. 10a). Moreover, density functional theory (DFT) calculations revealed that the interface energy between BCM and Zn(002) was 0.83×10^{-3} eV $Å^{-2}$, thereby facilitating preferential growth of Zn^{2+} along the (002) plane (Fig. 10b). Therefore, this mechanism of crystal orientation regulation provides new insights into optimizing Zn deposition behavior through the rational design of separators in achieving improved battery performance. Impressively, Zn||Zn symmetric cells using BCM separator demonstrated ultralong cycle lifespan exceeding 4000 h at 0.1 mAh cm^{-2} at a current density of 0.5 mA cm^{-2}. Besides, Cao et al.[40] developed a novel composite separator consisting of cellulose nanofibers and graphene oxide, which effectively induces Zn(002) deposition. This CG separator possessed a negative surface charge and abundant oxygen-containing functional groups with high Zn affinity. In the CG separator, the hexagonal lattice structure of graphene oxide aligns exceptionally well with the lattice parameter of the (002) crystal plane of Zn anode formed during zinc metal deposition, exhibiting a lattice mismatch of only 7.4% (Fig. 10c-e). Therefore, the CG separator facilitates the preferential growth of Zn along the (002) crystal plane, thereby ensuring uniform Zn deposition and suppressing the formation of Zn dendrites (Fig. 10f). These characteristics are crucial for enhancing the cycling stability and overall electrochemical performance of ZIBs. Accordingly, ultralong cycle life over 1750 h at 2 mA cm^{-2} and 400 h at 20 mA cm^{-2} was achieved for the Zn||Zn symmetric cells equipped with CG separator.

View Article Online
DOI: 10.1039/D5TA05279C

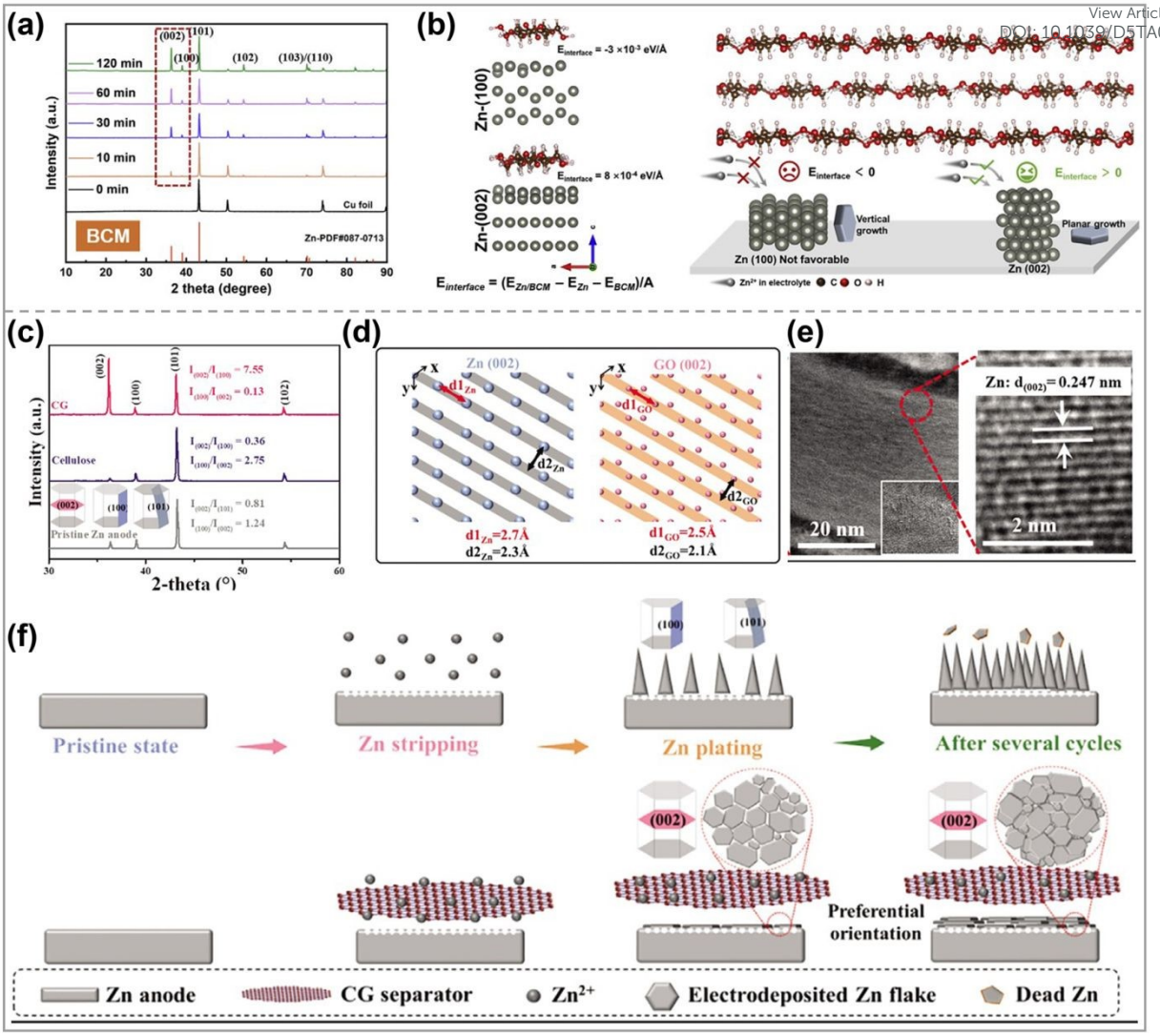

Fig. 10. (a) XRD patterns of plating Zn on Cu foil at different plating times with different BCM separators. (b) Side-view atomic structure between different crystal plane in Zn and BCM interface with corresponding calculated interfacial energy from DFT results, and schematic illustrations of manipulating crystallographic orientation. Reproduced with permission Ref. [28]. Copyright 2022, Elsevier. (c) Ex situ XRD patterns of Zn anodes after cycling. (d) Atomic arrangements of (002) plane of Zn and (002) plane of GO. (e) HRTEM images of the hexagonal zinc deposits with CG separator. (f) Schematic illustration of Zn stripping/plating with different separator. Reproduced with permission Ref. [40]. Copyright 2021, Wiley-VCH.

Recently, Yang et al.[91] reported that the novel FACNF separator, composed of industrial waste fly ash particles and cellulose nanofibers, can effectively regulate the Zn deposition behavior, thereby promoting preferential growth along the (002) crystal plane. To further elucidate the underlying mechanism, the research group employed DFT calculations to systematically investigate the adsorption energies between fly ash particles and Zn^{2+}/water molecules, as well as the interfacial energies between fly ash and various Zn crystal planes. The

View Article Online
DOI: 10.1039/D5TA05279C

theoretical results indicated that the interfacial energy between fly ash and the Zn (002) plane was positive (2 meV), suggesting negligible chemical interaction. In contrast, the interfacial energies for the Zn (100) and (101) planes are −100 meV and −20 meV, respectively, indicating strong chemical affinity between fly ash and these planes. Such a difference in interfacial energy drived Zn^{2+} to predominantly deposit along the (002) plane, thereby ensuring uniformZn deposition and effectively mitigating Zn dendrite formation. Consequently, Zn||Zn symmetric cells employing FACNF separators exhibited remarkable cycling stability (1600 h at 2 mA cm^{-2}, 1 mAh cm^{-2}). Therefore, biomass-based separators demonstrate dual modulation mechanisms that effectively regulate Zn deposition oriented along the (002) plane through rational structural design and interfacial engineering. Nevertheless, further research is required to comprehensively elucidate the microscopic mechanisms underlying separator-mediated regulation of Zn (002) crystal plane deposition. Moreover, crystal plane regulation strategies focus on guide Zn^{2+} ions to preferentially deposit along specific crystallographic orientations, thereby inhibiting their disordered and random deposition across multiple crystal planes. Notably, the crystal plane regulation is not exclusively limited to promoting Zn deposition along the (002). Therefore, further investigations are necessary to develop biomass-based separators to regulate the uniform Zn deposition on targeted crystal planes.

4.2 Optimize the Solvation Structure of Hydrated Zn^{2+}

Generally, Zn^{2+} predominantly exists in a hydrated state ($Zn(H_2O)_6^{2+}$) in the electrolyte, which tends to induce various side reactions, including HER during the Zn deposition process. Consequently, optimizing the physicochemical characteristics of the biomass-based separator to facilitate efficient desolvation of Zn^{2+} is essential for improving the controllability and stability of Zn deposition behavior. For instance, Yang et al.[105] developed a hydrophilic BC membrane that effectively mitigates water-induced side reactions by modulating the activity of water molecules. To further elucidate the underlying mechanism, molecular dynamics (MD) simulations were employed to investigate the interaction between the BC membrane and water molecules. The simulation results demonstrated that the BC membrane forms robust robust hydrogen bonding interactions with water molecules, thereby facilitating their transition from a free state to a bound state (Fig. 11a-c). Owing to its abundance of hydroxyl groups, the BC membrane exhibited strong hydrophilicity and can bind with water molecules via hydrogen bonding, thereby converting free water (FW) into bound water (BW). Consequently, the BC membrane not only significantly reduces the reactivity of water molecules, but also enhances mechanical stability through the formation of a hydrogen bond network between polymer chains and water molecules, which effectively suppresses the formation of Zn dendrites (Fig.

View Article Online
DOI: 10.1039/D5TA05279C

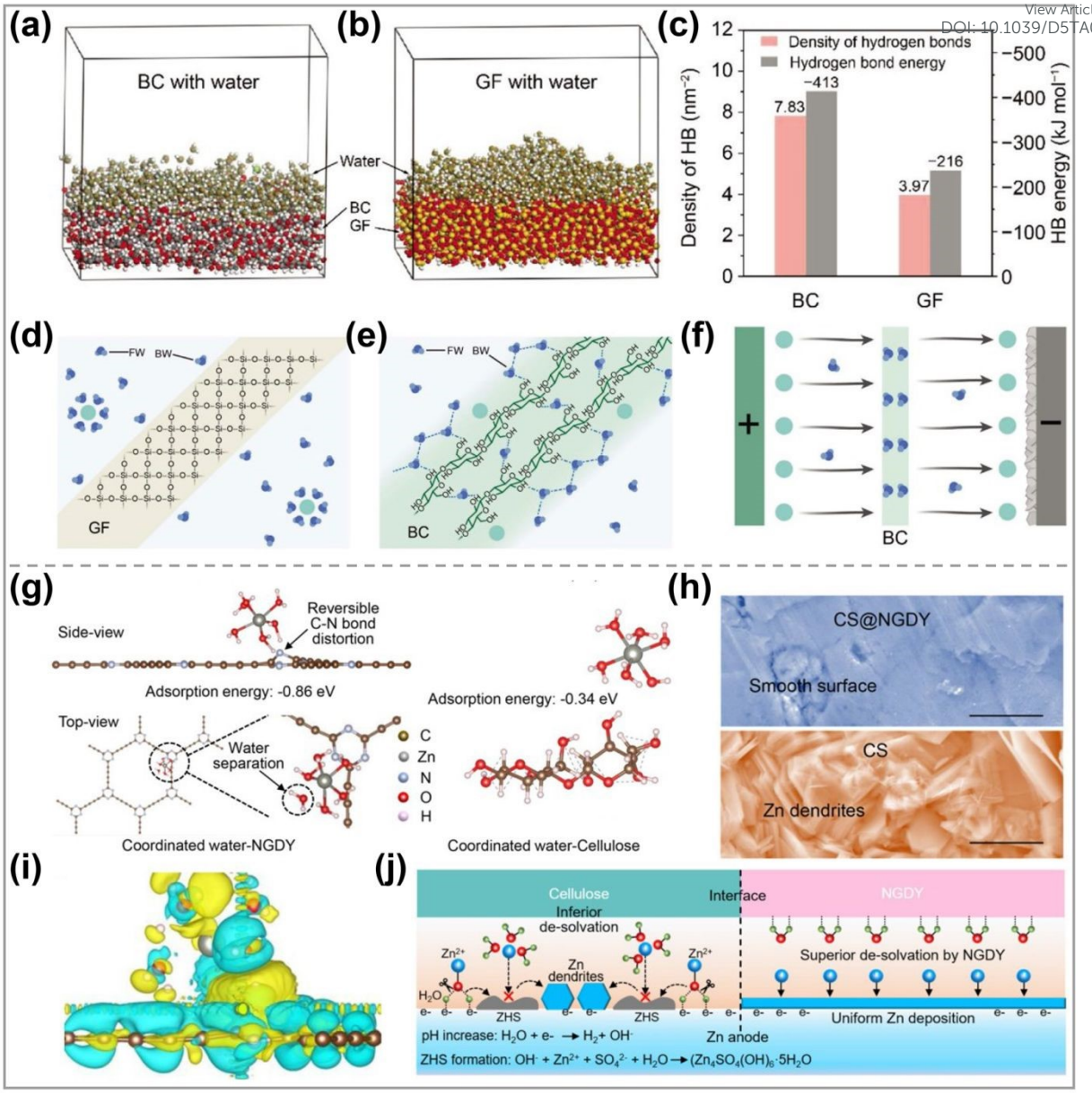

Fig. 11. (a) Snapshot of MD calculation for the interaction between BC and water. (b) Snapshot of MD calculation for the interaction between GF and water. (c) Density of interfacial hydrogen bonds and interfacial hydrogen bond energy of BC and GF with water from MD calculation. Schematic depiction of electrolyte state and the according Zn deposition: (d) GF separator and (e-f) BC membrane. Reproduced with permission Ref. [105]. Copyright 2023, Wiley-VCH. (g) Theoretical computation showing the interaction of the coordinated water in hydrated zin ions with NGDY and cellulose. (h) SEM images of Zn electrodes after cycling with NGDY and CS interfaces. (i) Isosurface charge density plot of NGDY-hydrated Zn^{2+}. (j) Schematic diagram demonstrating the NGDY-assisted stabilization of interface pH and suppressions of Zn dendrites. Reproduced with permission Ref. [39]. Copyright 2022, Wiley-VCH.

11d-f). Thanks to its excellent water molecule binding capability and the uniform distribution

View Article Online
DOI: 10.1039/D5TA05279C

of Zn^{2+}, the BC membrane significantly reduces local overpotential, prevents non-uniform deposition of Zn^{2+} on the electrode surface, and suppresses Zn dendrite growth. As a result, the Zn||Zn symmetric cells with the BC membrane cycled continuously for over 2000 h at 2 mA cm^{-2} and 2 mAh cm^{-2}. Zhi and co-workers[39] reported a NGDY interface that effectively stabilizes the interfacial pH by regulating the desolvation process of hydrated Zn^{2+} (Fig. 11g-j). In the NGDY, N atoms can attract water molecules coordinated with Zn^{2+}, thus significantly lowering the activation energy for desolvation. This underlying mechanism underlying direct electron transfers from the substrate to the empty orbitals of Zn^{2+}, thus bypassing the coordinated water molecules. As a result, the cleavage of O-H bonds is circumvented, thereby suppressing water decomposition and maintaining a stable interfacial pH. Moreover, DFT calculations revealed that NGDY exhibits significantly stronger binding with $Zn(H_2O)_6^{2+}$ compared to cellulose. This enhanced interaction significantly accelerates the desolvation process and promotes uniform Zn deposition through reversible structural distortion of the C=N bond and charge transfer-induced water splitting. In addition, the strong adsorption capability of NGDY also can facilitate Zn^{2+} desolvation through reducing their residence time on the electrode surface and enhancing transmission efficiency. Hence, the rapid desolvation process promotes rapid Zn^{2+} deposition while suppressing HER and other side reactions, which typically elevate the interfacial pH and induce Zn dendrite formation. Notably, the NGDY interface mitigates these issues by stabilizing the pH and promoting uniform Zn deposition. Consequently, the Zn||Zn symmetric cell with NGDY interface showed a long lifespan of 600 h at 3 mA cm^{-2}. Recently, Zhang et al.[101] fabricated a self-supporting, binder-free CNG membrane via ultrasonic dispersion techniques for ZIBs. The CNG membrane was self-assembled from graphene and cellulose nanocrystals through CH-π interactions. The porous structure of the CNG membrane provided abundant deposition sites for Zn^{2+}, thereby promoting their uniform distribution. Additionally, the CNG membrane demonstrated high selectivity for Zn^{2+} permeation while effectively shielding SO_4^{2-}. This selective ion transport mechanism ensures the homogeneous Zn deposition within the CNG membrane, significantly suppressing Zn dendrite formation. Owing to the strong hydrophilicity, the CNG membrane can adsorb water molecules, thus facilitating the removal of solvated water molecules surrounding Zn^{2+}. Meanwhile, the hydrophobic nature of graphene repels water molecules, further accelerating the desolvation process of Zn^{2+}. These synergistic effects facilitate partial desolvation of Zn^{2+} prior to reaching the Zn anode surface, thereby effectively mitigating water-induced corrosion reactions. Accordingly, ultralong cycle life of about 3000 h at 1 mA cm^{-2} and 0.5 mAh cm^{-2} was achieved for the Zn||Zn symmetric cells equipped with CNG membrane.

View Article Online
DOI: 10.1039/D5TA05279C

Indeed, the biomass-based separators typically exhibit multiple synergistic mechanisms during the optimization of zinc deposition and stabilization of the zinc anode. In addition to facilitating preferential Zn deposition along the (002) crystal plane and accelerating the desolvation kinetics, the following strategies can be employed to further improve the electrochemical performance of ZIBs: 1) Coating a Sn layer with excellent electrical conductivity and strong Zn affinity onto the cellulose separator surface effectively homogenizes the electric field distribution, thereby promoting smooth and uniform Zn deposition on the substrate;[99] 2) Incorporating CNF with high-dielectric-constant ZrO_2 induces Maxwell-Wagner polarization under an external electric field. This phenomenon not only regulates Zn^{2+} deposition but also significantly accelerates Zn^{2+} diffusion kinetics while repelling anion interference, thereby suppressing side reactions and stabilizing the Zn anode;[41] 3) A Janus separator with superior ion selectivity has been developed using sulfonated cellulose-modified graphene sheets. This separator repels SO_4^{2-} anions, immobilizes H^+ cations, and exclusively facilitates Zn^{2+} transport and deposition, thus substantially enhancing the cycling stability and Coulombic efficiency of ZIBs;[77] 4) Furthermore, it is crucial to prioritize the modulus, especially in the vertical direction, in the design of the separator, which significantly contributes to the inhibition of Zn dendrite growth. Therefore, it is also an effective strategy to prevent the formation of Zn dendrites by taking advantage of the mechanical inhibition effect of the separator.[50] In a word, biomass-based separators, including pure biomass, composite, and coating, have garnered considerable attention in ZIBs. By integrating multiple synergistic mechanisms, these separators effectively regulate Zn deposition behavior, resulting in significant enhancements in the electrochemical performance of ZIBs.

5. Summary and Outlook

In summary, we have outlined the recent advancements in biomass-based separators for application in aqueous ZIBs, focusing on fundamental requirements, structural configurations, preparation methods, and modification strategies. Among the critical components of ZIBs, the separator plays a vital role in ensuring the safe and efficient operation of the battery. Recently, biomass-based separators have emerged as promising candidates to replace conventional GF or polyolefin separators, owing to their hierarchical pore structures and abundant polar functional groups. These separators demonstrate enhanced ionic conductivity, thermal stability, mechanical strength, and environmental sustainability. Notably, biomass-based separators possess unique structural and functional advantages that facilitate effective regulation of Zn^{2+} flux, rapid Zn^{2+} transport, and suppression of Zn dendrites/side reactions. Furthermore, their

View Article Online
DOI: 10.1039/D5TA05279C

natural hydrophilicity and mechanical flexibility enhance electrode-electrolyte interfacial contact, contributing to improved cycling stability and rate performance. Despite these advancements, challenges remain in balancing scalability, cost-effectiveness, and performance metrics for practical applications. Based on the above analysis, future research should prioritize the following directions (Fig. 12):

(1) Integrating functional materials with biomass-based separators to develop composite multifunctional separators. By combining biomass with inorganic materials (e.g. graphene oxide, metal-organic frameworks (MOFs), and covalent organic frameworks (COFs)), the composite separators can be developed that exhibit synergistic effects, which significantly improve the mechanical and electrochemical properties. These frameworks are characterized by their tunable pore structures, high porosity, large specific surface areas, and ease of surface functionalization, making them ideal candidates for composite separator applications. In addition, MOFs/COFs can provide another channel for the movement of ions. However, the critical challenges involve achieving robust interfacial bonding between organic/inorganic phases, as well as addressing the high production costs. Future research should prioritize the design and modulation of interfaces to ensure optimal compatibility and performance.

(2) Exploring advanced techniques for the molecular-level functionalization and modification of biomass materials. By grafting various hydrophilic functional groups, such as −COOH and $-SO_3H$, the hydrophilicity, zincophilicity, and ionic conductivity of the biomass-based separators can be significantly enhanced. This modification not only facilitates rapid ion transport but also regulates the Zn deposition, thereby suppressing Zn dendrite growth and HER. Nevertheless, the introduction of these functional groups may disrupt the hydrogen bonding network within the biomass structure, potentially decreasing mechanical strength and structural stability. Advanced crosslinking strategies, such as aldehyde-assisted bridging, chemical grafting with physical entanglement, or radiation-induced polymerization, require in-depth investigation to reconcile this trade-off by reconstructing 3D hierarchical architectures. Future research should focus on developing machine learning-guided modification protocols and establishing structure-property relationships at electrode-separator interfaces to achieve precise control over functional group distribution.

(3) Deepening the insight into operational mechanisms of biomass-based separators. Current investigations into biomass-based separators for ZIBs predominantly emphasize material characterization, while comprehensive theoretical and mechanistic studies remain barely

View Article Online
DOI: 10.1039/D5TA05279C

explored. This limitation hinders the systematic selection and optimization of separator materials, resulting in a fragmented understanding of their operational mechanisms. Therefore, it is imperative to employ operando characterization and theoretical calculations to decouple the operational mechanisms. Future research should prioritize the integration of theoretical tools, such as DFT calculations and finite element simulations, to elucidate ion transport kinetics, interfacial interactions, and structure-property relationships at atomic/molecular levels. Additionally, multi-physics simulations coupling mechanical, electric, and ionic fields are essential for decoding dynamic processes, including pore-mediated ion migration and stress distribution under cycling conditions. By deepening the mechanism research, researchers can better interpret the microscopic interactions of biomass materials and the multi-field migration of ions, providing insights into discovering superior materials.

(4) Developing multifunctional and intelligent separators based on biomass materials. The safety and durability of ZIBs have gained significant attention due to the increasing demand for high energy density and fast charge/discharge rates. The unique advantages of ZIBs enable their use in practical applications under severe operating conditions, such as high current density and extreme temperatures. These conditions can exacerbate side reactions, including anodic dissolution, passivation, dendrite growth, and HER. Biomass materials offer unique opportunities to develop multifunctional separators for addressing these harsh operating conditions. Through the use of machine learning, we can rapidly screen and optimize separator designs, thus accelerating the intelligent development of these biomass materials. Furthermore, it is an important direction for developing biomass-based separators with self-repairability, which can repair mechanical cracks during cycling, extending battery lifespan. Future research should focus on the synergy between the intrinsic properties of natural macromolecules and their engineered functionalities.

(5) Mass production of cost-effective biomass-based separators. Transitioning from laboratory-scale prototypes to industrial production requires the development of cost-effective and sustainable fabrication methods. Currently, biomass-based separators frequently depend on energy-intensive processing methods (e.g., TEMPO oxidation for nanocellulose) or expensive modifiers. Therefore, it is necessary to explore low-cost, high-yield extraction methods, such as enzymatic hydrolysis or deep eutectic solvent/ionic liquids-assisted purification, to dissolve and regenerate biopolymers. Regarding preparation processes, there is a need to develop low-cost and efficient

View Article Online
DOI: 10.1039/D5TA05279C

manufacturing techniques for biomass-based separators. In the future, collaborative efforts with industry to optimize roll-to-roll manufacturing or 3D printing will be key to accelerating commercialization.

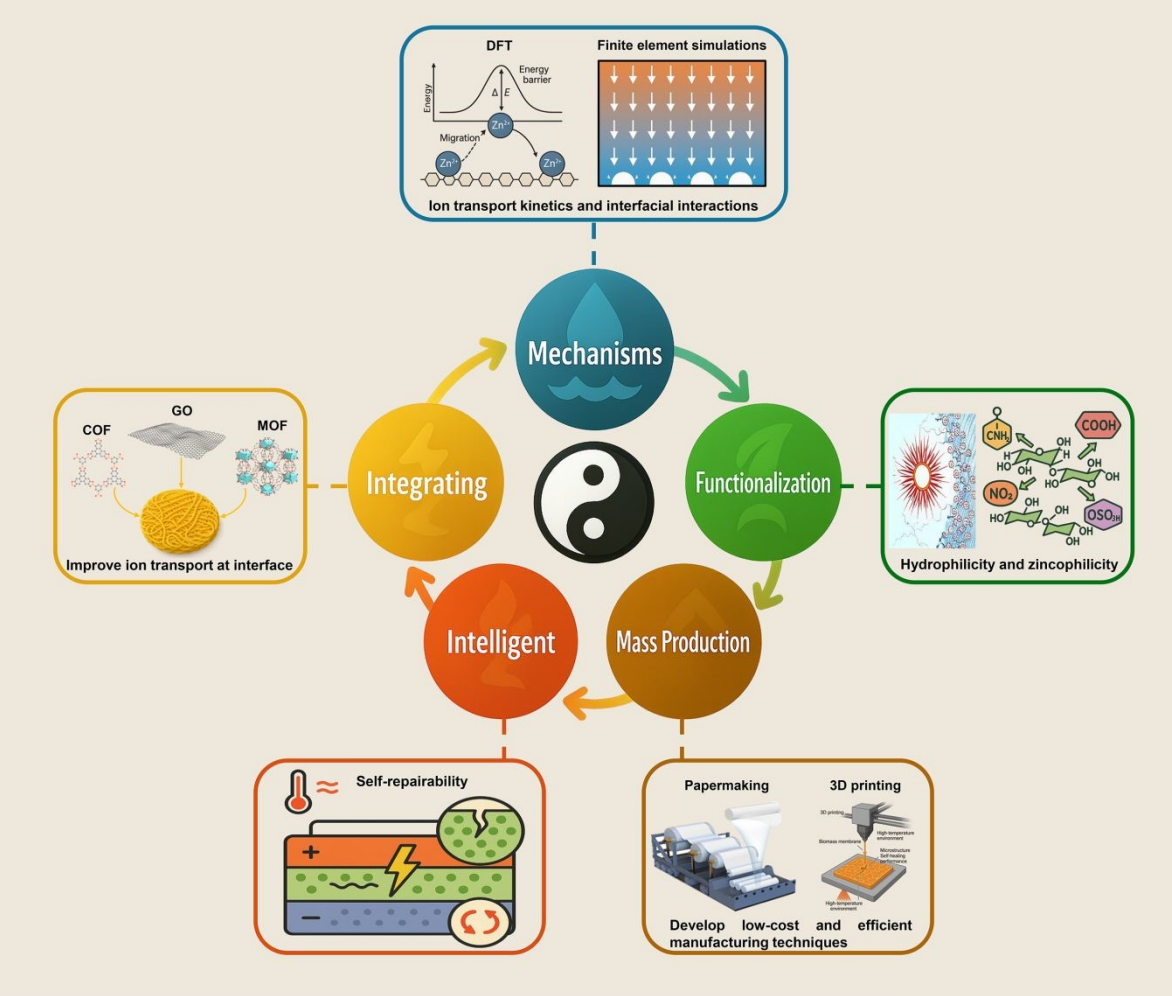

Fig. 12. Schematic illustration of the future directions of biomass-based separators for ZIBs.

Acknowledgements

We are grateful for the financial support by National Natural Science Foundation of China (Grant Nos. 32301533 and 32401519), China Postdoctoral Science Foundation (Grant No. 2023M732021), Guangzhou Basic and Applied Basic Research Foundation (Grant No. 2024A04J3413), and Guangdong Basic and Applied Basic Research Foundation (Grant No. 2025A1515011107).

View Article Online
DOI: 10.1039/D5TA05279C

References

1. L. Tang, H. Peng, J. Kang, H. Chen, M. Zhang, Y. Liu, D. H. Kim, Y. Liu and Z. Lin, *Chem. Soc. Rev.*, 2024, **53**, 4877-4925.
2. M. Zhao, Y. Lv, Y. Xu, H. Yang, Z. Bo and J. Lu, *Nat. Commun.*, 2025, **16**, 2843.
3. C. Yang, J. Xia, C. Cui, T. P. Pollard, J. Vatamanu, A. Faraone, J. A. Dura, M. Tyagi, A. Kattan, E. Thimsen, J. Xu, W. Song, E. Hu, X. Ji, S. Hou, X. Zhang, M. S. Ding, S. Hwang, D. Su, Y. Ren, X.-Q. Yang, H. Wang, O. Borodin and C. Wang, *Nat. Sustain.*, 2023, **6**, 325-335.
4. Y. Li, X. Li, X. Peng, X. Yang, F. Kang and L. Dong, *Nano-Micro Lett.*, 2025, **17**, 268.
5. J. Li, H. Jia, S. Ma, L. Xie, X.-X. Wei, L. Dai, H. Wang, F. Su and C.-M. Chen, *ACS Energy Lett.*, 2023, **8**, 56-78.
6. Y. Zong, H. He, Y. Wang, M. Wu, X. Ren, Z. Bai, N. Wang, X. Ning and S. X. Dou, *Adv. Energy Mater.*, 2023, **13**, 2300403.
7. J. Chen, M. Chen, H. Ma, W. Zhou and X. Xu, *Energy Rev.*, 2022, **1**, 100005.
8. B. Li, Y. Zeng, W. Zhang, B. Lu, Q. Yang, J. Zhou and Z. He, *Sci. Bull.*, 2024, **69**, 688-703.
9. J. Ming, J. Guo, C. Xia, W. Wang and H. N. Alshareef, *Mater. Sci. Eng. R-Rep*, 2019, **135**, 58-84.
10. Y. Liang, D. Ma, N. Zhao, Y. Wang, M. Yang, J. Ruan, G. Yang, H. Mi, C. He and P. Zhang, *Adv. Funct. Mater.*, 2022, **32**, 2112936.
11. S. Liu, Q. Han, C. He, Z. Xu, P. Huang, L. Cai, H. Chen, H. Zheng, Y. Zhou, M. Wang, H. Tian, W.-Q. Han and H. Ying, *ACS Nano*, 2024, **18**, 25880-25892.
12. X. Yang, X. Nie, C. Tang, Y. Xiao, Q. Li, D. Yuan and M. Yao, *Nano Res.*, 2025, **18**, 94907031.
13. W. Yang, W. Yang, J. Zeng, Y. Chen, Y. Huang, J. Liu, J. Gan, T. Li, H. Zhang, L. Zhong and X. Peng, *Prog. Mater. Sci.*, 2024, **144**, 101264.
14. Z. Fan, X. Chen, J. Shi, H. Nie, X. Zhang, X. Zhou, X. Xie and Z. Xue, *Nano-Micro Lett.*, 2025, **17**, 128.
15. Z. Xue, D. Zhu, M. Shan, H. Wang, J. Zhang, G. Cui, Z. Hu, K. C. Gordon, G. Xu and M. Zhu, *Nano Today*, 2024, **55**, 102175.
16. L. Zuo, Q. Ma, P. Xiao, Q. Guo, W. Xie, D. Lu, X. Yun, C. Zheng and Y. Chen, *Adv. Mater.*, 2024, **36**, 2311529.
17. H. Li, D. Wu, J. Wu, L.-Y. Dong, Y.-J. Zhu and X. Hu, *Adv. Mater.*, 2017, **29**, 1703548.
18. C. M. Costa, Y.-H. Lee, J.-H. Kim, S.-Y. Lee and S. Lanceros-Méndez, *Energy Storage Mater.*, 2019, **22**, 346-375.
19. W. Böhnstedt, *J. Power Sources*, 2004, **133**, 59-66.
20. Y. Hu, P. Li, G. Lai, B. Lu, H. Wang, H. Cheng, M. Wu, F. Liu, Z.-M. Dang and L. Qu, *Nat. Commun.*, 2025, **16**, 2772.
21. H. Du, Z. Yi, H. Li, W. Lv, N. Hu, X. Zhang, W. Chen, Z. Wei, F. Shen and H. He, *Chem. Eur. J.*, 2024, **30**, e202303461.
22. L. Yang, M. Zhou, Y. Xie, X. Shen, S. Liang and G. Fang, *Energy Storage Mater.*, 2024, **67**, 103271.
23. D. Djian, F. Alloin, S. Martinet, H. Lignier and J. Y. Sanchez, *J. Power Sources*, 2007, **172**, 416-421.
24. X. Shan, Z. Song, H. Ding, L. Li, Y. Tian, A. P. Sokolov, M. Tian, K. Xu and P.-F. Cao, *Energy Environ. Sci.*, 2024, **17**, 8457-8481.
25. N. S. Grundish, C. D. Amos, A. Agrawal, H. Khani and J. B. Goodenough, *Adv. Funct. Mater.*, 2019, **29**, 1903550.
26. H. Peng, L. Xiao, K. Sun, G. Ma, G. Wei and Z. Lei, *J. Power Sources*, 2019, **435**, 226800.
27. E. Lizundia, C. M. Costa, R. Alves and S. Lanceros-Méndez, *Carbohydr. Polym. Technol. Appl.*, 2020, **1**, 100001.

28. Y. Zhang, X. Li, L. Fan, Y. Shuai and N. Zhang, *Cell Rep. Phys. Sci.*, 2022, **3**, 100824.
29. Q. Wang, J. Zhao, J. Zhang, M. Li, F. Tan, X. Xue, Z. Sui, Y. Zou, X. Zhang, W. Zhang and C. Lu, *Adv. Funct. Mater.*, 2024, **34**, 2405957.
30. Y. Fang, X. Xie, B. Zhang, Y. Chai, B. Lu, M. Liu, J. Zhou and S. Liang, *Adv. Funct. Mater.*, 2022, **32**, 2109671.
31. W. Liu, S. Zhao, J. Lin, Y. Yang, Y. Chen and G. Zeng, *Int. J. Biol. Macromol.*, 2025, **306**, 141326.
32. W. Chen, L. Zhang, C. Liu, X. Feng, J. Zhang, L. Guan, L. Mi and S. Cui, *ACS Appl. Mater. Interfaces*, 2018, **10**, 23883-23890.
33. X. Ge, W. Zhang, F. Song, B. Xie, J. Li, J. Wang, X. Wang, J. Zhao and G. Cui, *Adv. Funct. Mater.*, 2022, **32**, 2200429.
34. Q. Xu, Q. Kong, Z. Liu, X. Wang, R. Liu, J. Zhang, L. Yue, Y. Duan and G. Cui, *ACS Sustain. Chem. Eng.*, 2014, **2**, 194-199.
35. X. Zhao, H. Zhou, V. S. Sikarwar, M. Zhao, A.-H. A. Park, P. S. Fennell, L. Shen and L.-S. Fan, *Energy Environ. Sci.*, 2017, **10**, 1885-1910.
36. P. Chen, X. Lin, B. Yang, Y. Gao, Y. Xiao, L. Li, H. Zhang, L. Li, Z. Zheng, J. Wang and S. Chou, *Adv. Funct. Mater.*, 2024, **34**, 2409368.
37. T.-W. Zhang, T. Tian, B. Shen, Y.-H. Song and H.-B. Yao, *Compos. Commun.*, 2019, **14**, 7-14.
38. S. Yang, Y. Zhang, Y. Zhang, J. Deng, N. Chen, S. Xie, Y. Ma and Z. Wang, *Adv. Funct. Mater.*, 2023, **33**, 2304280.
39. Q. Yang, L. Li, T. Hussain, D. Wang, L. Hui, Y. Guo, G. Liang, X. Li, Z. Chen, Z. Huang, Y. Li, Y. Xue, Z. Zuo, J. Qiu, Y. Li and C. Zhi, *Angew. Chem. Int. Ed.*, 2022, **61**, e202112304.
40. J. Cao, D. Zhang, C. Gu, X. Wang, S. Wang, X. Zhang, J. Qin and Z.-S. Wu, *Adv. Energy Mater.*, 2021, **11**, 2101299.
41. J. Cao, D. Zhang, C. Gu, X. Zhang, M. Okhawilai, S. Wang, J. Han, J. Qin and Y. Huang, *Nano Energy*, 2021, **89**, 106322.
42. Z. Zheng, S. Guo, M. Yan, Y. Luo and F. Cao, *Adv. Mater.*, 2023, **35**, 2304667.
43. H. Zhang, J. Li, H. Ren, J. Wang, Y. Gong, B. Wang, D. Wang, H. Liu and S. Dou, *iScience*, 2024, **27**, 110237.
44. X. Zhang, S. Yang and Z. Wang, *Chem. Eng. J.*, 2023, **466**, 143312.
45. V. Deimede and C. Elmasides, *Energy Technol.*, 2015, **3**, 453-468.
46. M. Xiong, H. Tang, Y. Wang and M. Pan, *Carbohydr. Polym.*, 2014, **101**, 1140-1146.
47. J. Zhang, L. Yue, Q. Kong, Z. Liu, X. Zhou, C. Zhang, Q. Xu, B. Zhang, G. Ding, B. Qin, Y. Duan, Q. Wang, J. Yao, G. Cui and L. Chen, *Sci. Rep.*, 2014, **4**, 3935.
48. S. C. Mun and J. H. Won, *Front. Energy Res.*, 2022, **10**, 928179.
49. D. Zhao, Y. Zhu, W. Cheng, W. Chen, Y. Wu and H. Yu, *Adv. Mater.*, 2021, **33**, 2000619.
50. H. Ma, H. Chen, M. Chen, A. Li, X. Han, D. Ma, P. Zhang and J. Chen, *Nat. Commun.*, 2025, **16**, 1014.
51. L. Zhang, Z. Liu, G. Cui and L. Chen, *Prog. Polym. Sci.*, 2015, **43**, 136-164.
52. R. J. Moon, A. Martini, J. Nairn, J. Simonsen and J. Youngblood, *Chem. Soc. Rev.*, 2011, **40**, 3941-3994.
53. W. Chen, H. Yu, S.-Y. Lee, T. Wei, J. Li and Z. Fan, *Chem. Soc. Rev.*, 2018, **47**, 2837-2872.
54. W. Yang, W. Yang, R. Zou, Y. Huang, H. Lai, Z. Chen and X. Peng, *Carbon Energy*, 2023, **5**, e203.
55. W. Zhou, M. Chen, Q. Tian, J. Chen, X. Xu and C.-P. Wong, *Energy Storage Mater.*, 2022, **44**, 57-65.
56. J. Fu, H. Wang, P. Xiao, C. Zeng, Q. Sun and H. Li, *Energy Storage Mater.*, 2022, **48**, 191-191f.

57. C. Cheng, R. Yang, Y. Wang, D. Fu, J. Sheng and X. Guo, *Carbohydr. Polym.*, 2023, **304**, 120489.
58. J. Ma, X. Shi, Z. Wang, L. Zhou, X. Liu, X. Lu and Z. Jiang, *Adv. Mater.*, 2024, **36**, 2406429.
59. C. Xi, Y. Xiao, C. Yang, M. Li, L. Li, Y. Chao, L. Li, C. He and Y. Yu, *J. Mater. Chem. A.*, 2023, **11**, 6522-6529.
60. Z. Zheng, S. Yan, Y. Zhang, X. Zhang, J. Zhou, J. Ye and Y. Zhu, *Chem. Eng. J.*, 2023, **475**, 146314.
61. L. Wang, F. Wang, Z. Ding, Y. Liu, Z. Zhang, C. Yang, K. P. Loh and Q.-H. Yang, *Green Energy Environ.*, 2024, **9**, 771-776.
62. P. Sheth, D. Patil, B. Kandasubramanian and N. Mayilswamy, *Polym. Bull.*, 2024, **81**, 15319-15348.
63. M. B. Arif, E. Yulianti, Q. Sabrina, S. Sudaryanto, S. T. C. Ndruru and M. Ghozali, *Polymer*, 2025, **323**, 128181.
64. J. Guo, Y. Wang, S. Li, Y. Meng, Y. Qin, L. Jiang, H. Huang and L. Shen, *J. Alloys Compd.*, 2023, **967**, 171708.
65. X. Yang, W. Wu, Y. Liu, Z. Lin and X. Sun, *Chem. Eng. J.*, 2022, **450**, 137902.
66. Z. Meng, Y. Jiao and P. Wu, *Angew. Chem. Int. Ed.*, 2023, **135**, e202307271.
67. H. Li, S. Askari, A. Kulachenko, M. Ek and O. Sevastyanova, *Int. J. Biol. Macromol.*, 2025, **290**, 138711.
68. D. Yuan, W. Manalastas Jr, L. Zhang, J. J. Chan, S. Meng, Y. Chen and M. Srinivasan, *ChemSusChem*, 2019, **12**, 4889-4900.
69. Z. Li, L. Ye, G. Zhou, W. Xu, K. Zhao, X. Zhang, S. Hong, T. Ma, M.-C. Li and C. Liu, *Chem. Eng. J.*, 2023, **457**, 141160.
70. C. Liedel, *ChemSusChem*, 2020, **13**, 2110-2141.
71. Z. Xue, T. Zhang, X. Li, F. Wang, G. Xu and M. Zhu, *Angew. Chem. Int. Ed.*, 2025, **64**, e202415283.
72. Y. Zhang, Z. Liu, X. Li, L. Fan, Y. Shuai and N. Zhang, *Adv. Energy Mater.*, 2023, **13**, 2302126.
73. S. Ou, J. Zheng, X. Chen, R. Li, Z. Yuan, S. Liu, Y. Niu, M. An, G. Zhou and Y. Yamauchi, *Energy Environ. Sci.*, 2025, **18**, 5457-5469.
74. Y.-Y. Sun, L. Yan, Q. Zhang, T.-B. Wang, Y.-C. Zha, L. Fan and H.-F. Jiang, *J. Colloid Interface Sci.*, 2023, **641**, 610-618.
75. W. Yan, J. Xian, S. Huang, Y. Leng, Q. Liu, T. Xiao, Y. Zhao, P. Yang and Y. Wu, *Energy Storage Mater.*, 2025, **76**, 104150.
76. W. Zhou, M. Yang, M. Chen, G. Zhang, X. Han, J. Chen, D. Ma and P. Zhang, *Adv. Funct. Mater.*, 2024, **34**, 2315444.
77. X. Zhang, J. Li, K. Qi, Y. Yang, D. Liu, T. Wang, S. Liang, B. Lu, Y. Zhu and J. Zhou, *Adv. Mater.*, 2022, **34**, 2205175.
78. W. Yang, W. Yang, Y. Huang, Y. Wu, X. Ma, L. Dong and X. Peng, *Energy Storage Mater.*, 2025, **80**, 104436.
79. J. Cao, D. Zhang, R. Chanajaree, D. Luo, X. Yang, X. Zhang and J. Qin, *Chem. Eng. J.*, 2024, **480**, 147980.
80. Y. Lei, Q. Li, Q. Liu, Y. Zeng, J. Li, W. Huang, F. Wang, S. Zhong and D. Yan, *Chem. Eng. J.*, 2024, **479**, 147846.
81. S. Xu, Z. Sun, D. Wei, L. Shao, M. Wang, Z. Wang, J. Zhang, T. Zhang, G. Liu and J. Cui, *J. Membr. Sci.*, 2024, **712**, 123230.
82. Y. Luo, Y. Yang, Y. Tao, D. Huang, B. Huang and H. Chen, *ACS Appl. Energy Mater.*, 2021, **4**, 14599-14607.
83. H. Qin, W. Chen, W. Kuang, N. Hu, X. Zhang, H. Weng, H. Tang, D. Huang, J. Xu and H. He, *Small*, 2023, **19**, 2300130.

84. S. Zheng, X. Yang, D. Chen, S. Huang, C. Zheng, H. Zhong, W. Zhang, X. Xiang, N. Zhang, Y. Sun and L. Liu, *Small*, 2025, **21**, 2411463.
85. X. Liu, F. Kong, Z. Wang, M. Ren, C. Qiao, W. Liu, J. Yao, C. Zhang and H. Zhao, *Scr. Mater.*, 2023, **233**, 115520.
86. P. Woottapanit, C. Yang, J. Cao, W. Limphirat, S. Saneewons na ayuttaya, X. Zhang, P. Wangyao and J. Qin, *ACS Appl. Energy Mater.*, 2023, **6**, 10578-10584.
87. J. Niu, J. Cao, X. Zhang, D. Zhang, C. Yang, K. Lolupiman, Z. Zeng, X. Zhang and J. Qin, *ACS Appl. Energy Mater.*, 2024, **7**, 7496-7504.
88. M. Wang, Z. Dai, C. Yang, D. Xu, X. Zhang, L. Que, X. Zhang and J. Qin, *Mater. Today Energy*, 2024, **46**, 101736.
89. W. Xu, X. Liao, W. Xu, K. Zhao, G. Yao and Q. Wu, *Adv. Energy Mater.*, 2023, **13**, 2300283.
90. S.-J. Lee, J.-H. Choi, I. Hwang, M.-H. Ryu, K.-N. Jung, H.-g. Cho, J. In Lee and G. Park, *Electrochem. Commun.*, 2025, **172**, 107882.
91. C. Yang, P. Woottapanit, Y. Yue, S. Geng, J. Cao, X. Zhang, G. He and J. Qin, *Small*, 2024, **20**, 2311203.
92. H. Ma, J. Yu, M. Chen, X. Han, J. Chen, B. Liu and S. Shi, *Adv. Funct. Mater.*, 2023, **33**, 2307384.
93. Y. Zhang, Z. Zeng, S. Yang, Y. Zhang, Y. Ma and Z. Wang, *Energy Storage Mater.*, 2023, **57**, 557-567.
94. L. Li, J. Peng, X. Jia, X. Zhu, B. Meng, K. Yang, D. Chu, N. Yang and J. Yu, *Electrochim. Acta*, 2022, **430**, 141129.
95. J. Guo, Y. Wang, S. Li, Y. Qin, Y. Meng, L. Jiang, H. Huang and L. Shen, *J. Power Sources*, 2023, **580**, 233392.
96. Y. Yang, T. Chen, B. Yu, M. Zhu, F. Meng, W. Shi, M. Zhang, Z. Qi, K. Zeng and J. Xue, *Chem. Eng. J.*, 2022, **433**, 134077.
97. K. Zhang, S. Xie, J. Liang, Z. Zheng, Y. Li and L. Dong, *J. Membr. Sci.*, 2025, **722**, 123876.
98. J. Wang, Y. Zhang, X. Peng, W. Gong, D. Ye and J. Xu, *J. Energy Storage*, 2024, **93**, 112386.
99. Z. Hou, Y. Gao, H. Tan and B. Zhang, *Nat. Commun.*, 2021, **12**, 3083.
100. Y. Li, X. Peng, X. Li, H. Duan, S. Xie, L. Dong and F. Kang, *Adv. Mater.*, 2023, **35**, 2300019.
101. X. Zhang, J. Li, D. Liu, M. Liu, T. Zhou, K. Qi, L. Shi, Y. Zhu and Y. Qian, *Energy Environ. Sci.*, 2021, **14**, 3120-3129.
102. Z. Zhang, Y. Li, X. Yin, S. Li, B. Li, N. Zhao, J. Zhu, L. Dai, L. Wang, Z. He and Z. Feng, *Green Energy Environ.*, 2025, DOI: 10.1016/j.gee.2025.03.010.
103. J. Wang, Z. Xu, Q. Zhang, X. Song, X. Lu, Z. Zhang, A. J. Onyianta, M. Wang, M.-M. Titirici and S. J. Eichhorn, *Adv. Mater.*, 2022, **34**, 2206367.
104. T. Wang, Q. Liu, J. Zhou, X. Wang and B. Lu, *Adv. Energy Mater.*, 2022, **12**, 2202357.
105. X. Yang, Z. Zhang, M. Wu, Z. P. Guo and Z. J. Zheng, *Adv. Mater.*, 2023, **35**, 2303550.

View Article Online
DOI: 10.1039/D5TA05279C

Data Availability Statements

No primary research results, software or code have been included and no new data were generated or analysed as part of this review.